**Figure 8.** Calpain-10 activation in AD pathology and its implication in neuronal Aβ secretion. *A–D*) Triple fluorescence microscopy illustrating colocalization of calpain-10 (*A*) and SNAP-25 (*B*) in the periphery of a FSB-stained plaque (*C*; 3-channel image shown in *D*) in the neocortex of a 24-mo-old APP-Tg mouse. *E–H*) Double-fluorescence microscopic views of senile plaques in the hippocampus of a patient with AD. Calpain-10 (*E*) and SNAP-10 (*G*) immunolabeling were merged onto FSB-stained plaques (*F, H*). *I, J*) A hippocampal slice from a patient with AD double labeled with anti-calpain-10 antibody (*I*) and FSB (*J*), demonstrating calpain-10 activation coexistent with neurofibrillary tangles and neuropil threads. Scale bars = 50 μm (*A–H*); 25 μm (*I, J*).
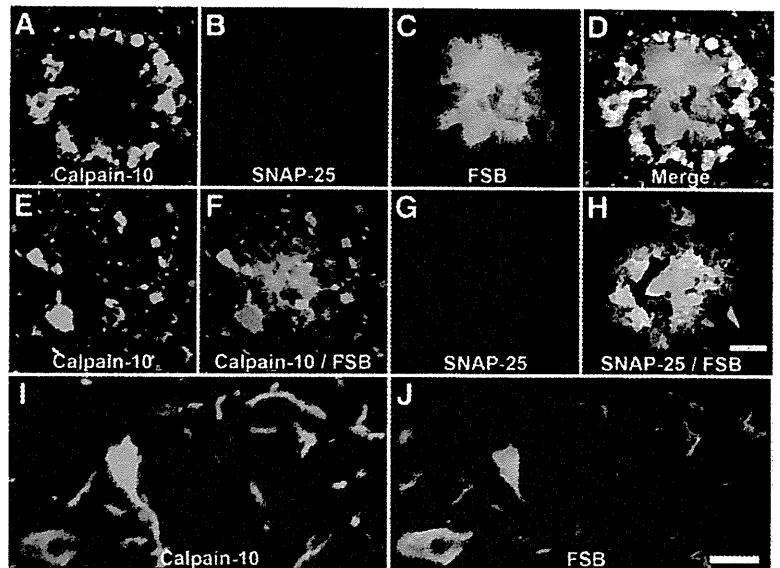
phic changes of apical dendrites in CS-KO/APP-Tg mice at 5–6 mo of age.

The present study has also implicated calpain in the radical morphological disruptions that occur downstream of amyloidogenesis. The most notable consequences for neuronal structure include disregulation of neurite extension and synaptic formation, in agreement with the fact that disrupted neuronal connectivity and aberrant neuritic sprouting occur in AD brains (55, 56). Moreover, an axonal tracing study in APP23 mice has revealed that ectopic growth of axons and pathological enlargement of synaptic termini are tightly associated with amyloid deposition (57). It is of particular interest that the site of calpain activation in the APP-Tg mice coincided with GABA$_A$ receptor expression. GABA$_A$ receptors are known to emerge early in the development of the central nervous system and are concentrated in the growth cone. Experiments using isolated growth cones have indicated that the activation of GABA$_A$ receptors in the growth cone membrane is mechanistically linked to calcium influx *via* L-type voltage-sensitive calcium channels (33), leading to calcium-dependent degradation of cytoskeletal constituents by calpain (58). Therefore, the involvement of GABA$_A$ receptors and calpain in ectopic neurite outgrowth and the generation of aberrant synaptic termini may partially recapitulate the molecular profile of developing neuronal growth cones. However, GABA$_A$ receptor activation alone does not seem to account for the neuropathology of the mutant mice.

We also observed caspase activation in presynaptic, GAP43-immunoreactive compartments in the brains of APP-Tg and crossbred mice. GAP43 labeling is consistently observed in dystrophic termini surrounding plaque lesions (57), justifying the view that activation of caspase may lead to an increase in the dynamics of presynaptic cytoskeletal reconfiguration. It has been suggested that crosstalk may exist between calpain and caspase (59). Caspase-12 is known to be activated by

calpain (60), and suppression of excitotoxicity-induced calpain activation attenuates caspase activity (18). In addition, caspase-mediated cleavage of CS leads to increased calpain activity (61). Although we observed little overlap between the localization of 150kf/136kf and Clact32 in the brains of patients with AD and APP-Tg mice, it is likely that activation of calpain-10 and caspases occurs concurrently in presynaptic terminals. However, overexpression or deficiency of CS did not alter the ratio of caspase activation to Aβ load in the APP-Tg mice. Therefore, we postulate that caspase activation is not an essential requirement for calpain-mediated neuropathology following Aβ accumulation. However, there remains a possibility that caspases may be involved in AD pathology independent of the calpain-CS system.

The results that we obtained from crossbred mice argue for the consideration of agents that act on the calpain-CS system in therapeutic approaches to AD. Taken together with the fact that CS is decreased in AD brains (62), the present findings in CS-KO/APP-Tg mice strongly support a primary role of the calpain-CS system in the modulation of AD pathologies. Furthermore, the CS overexpression-mediated attenuation of Aβ deposition and neuroglial degeneration in APP-Tg mice highlights the potential of regulating the calpain-CS system in interventions targeting the neuropathological devastation of AD. This strategy could also be beneficial in maintaining neuronal function. It would be of considerable interest to determine whether truly calpain-specific inhibitors, which may become available in the near future, rescue the Aβ amyloidosis and related neuropathologies observed in APP-Tg and CS-KO/APP-Tg mice. Furthermore, the CS-KO/APP-Tg mice could prove of great value in preclinical testing of the efficacy and specificity of such compounds. The simplest experimental design would be to measure the average life span of groups of CS-KO/

APP-Tg mice receiving different treatments without having to perform neuropathological analyses. [FJ]

REFERENCES

1. Sturchler-Pierrat, C., Abramowski, D., Duke, M., Wiederhold, K. H., Mistl, C., Rothacher, S., Ledermann, B., Bürki, K., Frey, P., Paganetti, P. A., Waridel, C., Calhoun, M. E., Jucker, M., Probst, A., Staufenbiel, M., and Sommer, B. (1997) Two amyloid precursor protein transgenic mouse models with Alzheimer disease-like pathology. *Proc. Natl. Acad. Sci. U. S. A.* **94,** 13287–13292

2. Hardy, J., and Selkoe, D. J. (2002) The amyloid hypothesis of Alzheimer's disease: progress and problems on the road to therapeutics. *Science* **297,** 353–356

3. Saido, T. C., and Iwata, N. (2006) Metabolism of amyloid β peptide and pathogenesis of Alzheimer's disease: Towards pre-symptomatic diagnosis, prevention and therapy. *Neurosci. Res.* **54,** 235–253

4. Higuchi, M., Ishihara, T., Zhang, B., Hong, M., Andreadis, A., Trojanowski, J. Q., and Lee, V. M. (2002) Transgenic mouse model of tauopathies with glial pathology and nervous system degeneration. *Neuron* **35,** 433–446

5. Goll, D. E., Thompson, V. F., Li, H., Wei, W., and Cong, J. (2003) The calpain system. *Physiol. Rev.* **83,** 731–801

6. Hayashi, T., and Abe, K. (2004) Ischemic neuronal cell death and organellae damage. *Neurol. Res.* **26,** 827–834

7. Raghupathi, R. (2004) Cell death mechanisms following traumatic brain injury. *Brain Pathol.* **14,** 215–222

8. Mattson, M. P., and Chan, S. L. (2003) Neuronal and glial calcium signaling in Alzheimer's disease. *Cell Calcium* **34,** 385–397

9. Glabe, C. G., and Kayed, R. (2006) Common structure and toxic function of amyloid oligomers implies a common mechanism of pathogenesis. *Neurology* **66,** S74–78

10. Gomez-Ramos, A., Diaz-Hernandez, M., Cuadros, R., Hernandez, F., and Avila, J. (2006) Extracellular tau is toxic to neuronal cells. *FEBS Lett.* **580,** 4842–4850

11. Kuchibhotla, K. V., Goldman, S. T., Lattarulo, C. R., Wu, H. Y., Hyman, B. T., and Bacskai, B. J. (2008) Aβ plaques lead to aberrant regulation of calcium homeostasis *in vivo* resulting in structural and functional disruption of neuronal networks. *Neuron* **59,** 214–225

12. Busche, M. A., Eichhoff, G., Adelsberger, H., Abramowski, D., Wiederhold, K. H., Haass, C., Staufenbiel, M., Konnerth, A., and Garaschuk, O. (2008) Clusters of hyperactive neurons near amyloid plaques in a mouse model of Alzheimer's disease. *Science* **321,** 1686–1689

13. Liu, J., Liu, M. C., and Wang, K. K. (2008) Calpain in the CNS: from synaptic function to neurotoxicity. *Sci. Signal.* **1,** re1

14. Saito, K., Elce, J. S., Hamos, J. E., and Nixon, R. A. (1993) Widespread activation of calcium-activated neutral proteinase (calpain) in the brain in Alzheimer disease: a potential molecular basis for neuronal degeneration. *Proc. Natl. Acad. Sci. U. S. A.* **90,** 2628–2632

15. Nixon, R. A., Saito, K. I., Grynspan, F., Griffin, W. R., Katayama, S., Honda, T., Mohan, P. S., Shea, T. B., and Beermann, M. (1994) Calcium-activated neutral proteinase (calpain) system in aging and Alzheimer's disease. *Ann. N. Y. Acad. Sci.* **747,** 77–91

16. Wang, K. K. W., and Yuen, P. W. (1992) Calpain substrates, assay methods, regulation, and its inhibitory agents. In: *CALPAIN: Pharmacology and Toxicology of Calcium-dependent Protease* (Wang, K. K. W., and Yuen, P. W. eds) pp. 77–101, Taylor & Francis, Philadelphia

17. Takano, J., Tomioka, M., Tsubuki, S., Higuchi, M., Iwata, N., Itohara, S., Maki, M., and Saido, T. C. (2005) Calpain mediates excitotoxic DNA fragmentation via mitochondrial pathways in adult brains: evidence from calpastatin mutant mice. *J. Biol. Chem.* **280,** 16175–16184

18. Higuchi, M., Tomioka, M., Takano, J., Shirotani, K., Iwata, N., Masumoto, H., Maki, M., Itohara, S., and Saido, T. C. (2005) Distinct mechanistic roles of calpain and caspase activation in neurodegeneration as revealed in mice overexpressing their specific inhibitors. *J. Biol. Chem.* **280,** 15229–15237

19. Crews, F. T., Morrow, A. L., Criswell, H., and Breese, G. (1996) Effects of ethanol on ion channels. *Int. Rev. Neurobiol.* **39,** 283–367

20. Tomioka, M., Shirotani, K., Iwata, N., Lee, H. J., Yang, F., Cole, G. M., Seyama, Y., and Saido, T. C. (2002) In vivo role of caspases in excitotoxic neuronal death: generation and analysis of transgenic mice expressing baculoviral caspase inhibitor, p35, in postnatal neurons. *Brain Res. Mol. Brain Res.* **108,** 18–32

21. Higuchi, M., Iwata, N., Matsuba, Y., Sato, K., Sasamoto, K., and Saido, T. C. (2005) ^{19}F and ^{1}H MRI detection of amyloid β plaques in vivo. *Nat. Neurosci.* **8,** 527–533

22. DeMattos, R. B., Bales, K. R., Parsadanian, M., O'Dell, M. A., Foss, E. M., Paul, S. M., and Holtzman, D. M. (2002) Plaque-associated disruption of CSF and plasma amyloid-β (Aβ) equilibrium in a mouse model of Alzheimer's disease. *J. Neurochem.* **81,** 229–236

23. Iwata, N., Mizukami, H., Shirotani, K., Takaki, Y., Muramatsu, S., Lu, B., Gerard, N. P., Gerard, C., Ozawa, K., and Saido, T. C. (2004) Presynaptic localization of neprilysin contributes to efficient clearance of amyloid-β peptide in mouse brain. *J. Neurosci.* **24,** 991–998

24. Huang, S. M., Mouri, A., Kokubo, H., Nakajima, R., Suemoto, T., Higuchi, M., Staufenbiel, M., Noda, Y., Yamaguchi, H., Nabeshima, T., and Saido, T. C. (2006) Neprilysin-sensitive synapse-associated Aβ oligomers impair neuronal plasticity and cognitive function. *J. Biol. Chem.* **281,** 17941–17951

25. Yoshiyama, Y., Higuchi, M., Zhang, B., Huang, S. M., Iwata, N., Saido, T. C., Maeda, J., Suhara, T., Trojanowski, J. Q., and Lee, V. M. (2007) Synapse loss and microglial activation precede tangles in a P301S tauopathy mouse model. *Neuron* **53,** 337–351

26. Maeda, J., Ji, B., Irie, T., Tomiyama, T., Maruyama, M., Okauchi, T., Staufenbiel, M., Iwata, N., Ono, M., Saido, T. C., Suzuki, K., Mori, H., Higuchi, M., and Suhara, T. (2005) Longitudinal, quantitative assessment of amyloid, neuroinflammation, and anti-amyloid treatment in a living mouse model of Alzheimer's disease enabled by positron emission tomography. *J. Neurosci.* **27,** 10957–10968

27. Saido, T. C., Nagao, S., Shiramine, M., Tsukaguchi, M., Sorimachi, H., Murofushi, H., Tsuchiya, T., Ito, H., and Suzuki, K. (1992) Autolytic transition of μ-calpain as resolved by antibodies distinguishing between the pre- and post-autolysis forms. *J. Biochem.* **111,** 81–86

28. Saido, T. C., Yokota, M., Nagao, S., Yamaura, I., Tani, E., Tsuchiya, T., Suzuki, K., and Kawashima, S. (1993) Spatial resolution of fodrin proteolysis in postischemic brain. *J. Biol. Chem.* **268,** 25239–25243

29. Saido, T. C., Nagao, S., Shiramine, M., Tsukaguchi, M., Yoshizawa, T., Sorimachi, H., Ito, H., Tsuchiya, T., Kawashima, S., and Suzuki, K. (1994) Distinct kinetics of subunit autolysis in mammalian m-calpain activation. *FEBS Lett.* **346,** 263–267

30. Saido, T. C., Iwatsubo, T., Mann, D. M., Shimada, H., Ihara, Y., and Kawashima, S. (1995) Dominant and differential deposition of distinct β-amyloid peptide species, Aβ$_{N3(pE)}$, in senile plaques. *Neuron* **14,** 457–466

31. Taniguchi, S., Fujita, Y., Hayashi, S., Kakita, A., Takahashi, H., Murayama, S., Saido, T. C., Hisanaga, S., Iwatsubo, T., and Hasegawa, M. (2001) Calpain-mediated degradation of p35 to p25 in postmortem human and rat brains. *FEBS Lett.* **489,** 46–50

32. Koffie, R. M., Meyer-Luehmann, M., Hashimoto, T., Adams, K. W., Mielke, M. L., Garcia-Alloza, M., Micheva, K. D., Smith, S. J., Kim, M. L., Lee, V. M., Hyman, B. T., and Spires-Jones, T. L. (2009) Oligomeric amyloid β associates with postsynaptic densities and correlates with excitatory synapse loss near senile plaques. *Proc. Natl. Acad. Sci. U. S. A.* **106,** 4012–4017

33. Fukura, H., Komiya, Y., and Igarashi, M. (1996) Signaling pathway downstream of GABA$_A$ receptor in the growth cone. *J. Neurochem.* **67,** 1426–1434

34. Vosler, P. S., Brennan, C. S., and Chen, J. (2008) Calpain-mediated signaling mechanisms in neuronal injury and neurodegeneration. *Mol. Neurobiol.* **38,** 78–100

35. Roselli, F., Tirard, M., Lu, J., Hutzler, P., Lamberti, P., Livrea, P., Morabito, M., and Almeida, O. F. (2005) Soluble β-amyloid1–40 induces NMDA-dependent degradation of postsynaptic density-95 at glutamatergic synapses. *J. Neurosci.* **25,** 11061–11070

36. Lu, X., Rong, Y., and Baudry, M. (2000) Calpain-mediated degradation of PSD-95 in developing and adult rat brain. *Neurosci. Lett.* **286,** 149–153

37. Xu, W., Wong, T. P., Chery, N., Gaertner, T., Wang, Y. T., and Baudry, M. (2007) Calpain-mediated mGluR1 α truncation: A key step in excitotoxicity. *Neuron* **53,** 399–412

38. Fifre, A., Sponne, I., Koziel, V., Kriem, B., Yen Potin, F. T., Bihain, B. E., Olivier, J. L., Oster, T., and Pillot, T. (2006) Microtubule-associated protein MAP1A, MAP1B, and MAP2 proteolysis during soluble amyloid β-peptide-induced neuronal apoptosis. Synergistic involvement of calpain and caspase-3. *J. Biol. Chem.* **281,** 229–240

39. Kelly, B. L., and Ferreira, A. (2006) β-Amyloid-induced dynamin 1 degradation is mediated by *N*-methyl-D-aspartate receptors in hippocampal neurons. *J. Biol. Chem.* **281,** 28079–28089

40. Vanderklish, P. W., Krushel, L. A., Holst, B. H., Gally, J. A., Crossin, K. L., and Edelman, G. M. (2000) Marking synaptic activity in dendritic spines with a calpain substrate exhibiting fluorescence resonance energy transfer. *Proc. Natl. Acad. Sci. U. S. A.* **97,** 2253–2258

41. Mathews, P. M., Jiang, Y., Schmidt, S. D., Grbovic, O. M., Mercken, M., and Nixon, R. A. (2002) Calpain activity regulates the cell surface distribution of amyloid precursor protein. Inhibition of calpains enhances endosomal generation of β-cleaved C-terminal APP fragments. *J. Biol. Chem.* **277,** 36415–36424

42. Liang, B., Duan, B. Y., Zhou, X. P., Gong, J. X., and Luo, Z. G. (2010) Calpain activation promotes BACE1 expression, amyloid precursor protein processing, and amyloid plaque formation in a transgenic mouse model of Alzheimer disease. *J. Biol. Chem.* **285,** 27737–27744

43. Dong, Y., Tan, J., Cui, M. Z., Zhao, G., Mao, G., Singh, N., and Xu, X. (2006) Calpain inhibitor MDL28170 modulates Aβ formation by inhibiting the formation of intermediate Aβ46 and protecting Aβ from degradation. *FASEB J.* **20,** 331–333

44. Evans, J. S., and Turner, M. D. (2007) Emerging functions of the calpain superfamily of cysteine proteases in neuroendocrine secretory pathways. *J. Neurochem.* **103,** 849–859

45. Marshall, C., Hitman, G. A., Partridge, C. J., Clark, A., Ma, H., Shearer, T. R., and Turner, M. D. (2005) Evidence that an isoform of calpain-10 is a regulator of exocytosis in pancreatic β-cells. *Mol. Endocrinol.* **19,** 213–224

46. Díaz-Villaseñor, A., Burns, A. L., Salazar, A. M., Sordo, M., Hiriart, M., Cebrián, M. E., and Ostrosky-Wegman, P. (2008) Arsenite reduces insulin secretion in rat pancreatic beta-cells by decreasing the calcium-dependent calpain-10 proteolysis of SNAP-25. *Toxicol. Appl. Pharmacol.* **231,** 291–299

47. Cirrito, J. R., Yamada, K. A., Finn, M. B., Sloviter, R. S., Bales, K. R., May, P. C., Schoepp, D. D., Paul, S. M.,. Mennerick, S., and Holtzman, D. M. (2005) Synaptic activity regulates interstitial fluid amyloid-β levels *in vivo. Neuron* **48,** 913–922

48. Cirrito, J. R., Kang, J. E., Lee, J., Stewart, F. R., Verges, D. K., Silverio, L. M., Bu, G., Mennerick, S., and Holtzman, D. M. (2008) Endocytosis is required for synaptic activity-dependent release of amyloid-β *in vivo. Neuron* **58,** 42–51

49. Park, S. Y., and Ferreira, A. (2005) The generation of a 17 kDa neurotoxic fragment: an alternative mechanism by which tau mediates β-amyloid-induced neurodegeneration. *J. Neurosci.* **25,** 5365–5375

50. Noble, W., Olm, V., Takata, K., Casey, E., Mary, O., Meyerson, J., Gaynor, K., LaFrancois, J., Wang, L., Kondo, T., Davies, P., Burns, M., Veeranna Nixon, R., Dickson, D., Matsuoka, Y., Ahlijanian, M., Lau, L. F., Duff, K. (2003) Cdk5 is a key factor in tau aggregation and tangle formation *in vivo. Neuron* **38,** 555–565

51. Cruz, J. C., and Tsai, L. H. (2004) Cdk5 deregulation in the pathogenesis of Alzheimer's disease. *Trends Mol. Med.* **10,** 452–458

52. Higuchi, M., Lee, V. M., and Trojanowski, J. Q. (2002) Tau and axonopathy in neurodegenerative disorders. *Neuromolecular Med.* **2,** 131–150

53. Veeranna, Kaji, T., Boland, B., Odrljin, T., Mohan, P., Basavarajappa, B. S., Peterhoff, C., Cataldo, A., Rudnicki, A., Amin, N., Li, B. S., Pant, H. C., Hungund, B. L., Arancio, O., and Nixon, R. A. (2004) Calpain mediates calcium-induced activation of the Erk1,2 MAPK pathway and cytoskeletal phosphorylation in neurons: relevance to Alzheimer's disease. *Am. J. Pathol.* **165,** 759–805

54. Amadoro, G., Ciotti, M. T., Costanzi, M., Cestari, V., Calissano, P., and Canu, N. (2006) NMDA receptor mediates tau-induced neurotoxicity by calpain and ERK/MAPK activation. *Proc. Natl. Acad. Sci. U. S. A.* **103,** 2892–2897

55. Geddes, J. W., Anderson, K. J., and Cotman, C. W. (1986) Senile plaques as aberrant sprout-stimulating structures. *Exp. Neurol.* **94,** 767–776

56. Masliah, E., Mallory, M., Hansen, L., Alford, M., Albright, T., DeTeresa, R., Terry, R., Baudier, J., and Saitoh, T. (1991) Patterns of aberrant sprouting in Alzheimer's disease. *Neuron* **6,** 729–739

57. Phinney, A. L., Deller, T., Stalder, M., Calhoun, M. E., Frotscher, M., Sommer, B., Staufenbiel, M., and Jucker, M. (1999) Cerebral amyloid induces aberrant axonal sprouting and ectopic terminal formation in amyloid precursor protein transgenic mice. *J. Neurosci.* **19,** 8552–8559

58. Ohbayashi, K., Fukura, H., Inoue, H. K., Komiya, Y., and Igarashi, M. (1998) Stimulation of L-type Ca^{2+} channel in growth cones activates two independent signaling pathways. *J. Neurosci. Res.* **51,** 682–696

59. O'Donovan, C. N., Tobin, D., and Cotter, T. G. (2001) Prion protein fragment PrP-(106–126) induces apoptosis via mitochondrial disruption in human neuronal SH-SY5Y cells. *J. Biol. Chem.* **276,** 43516–43523

60. Nakagawa, T., and Yuan, J. (2000) Cross-talk between two cysteine protease families. Activation of caspase-12 by calpain in apoptosis. *J. Cell Biol.* **150,** 887–894

61. Porn-Ares, M. I., Samali, A., and Orrenius, S. (1998) Cleavage of the calpain inhibitor, calpastatin, during apoptosis. *Cell Death Differ.* **5,** 1028–1033

62. Nilsson, E., Alafuzoff, I., Blennow, K., Blomgren, K., Hall, C. M., Janson, I., Karlsson, I., Wallin, A., Gottfries, C. G., and Karlsson, J. O. (1990) Calpain and calpastatin in normal and Alzheimer-degenerated human brain tissue. *Neurobiol. Aging* **11,** 425–431

Calpastatin, an endogenous calpain–inhibitor protein, regulates the cleavage of the Cdk5 activator p35 to p25

Ko Sato,* Seiji Minegishi,* Jiro Takano,† Florian Plattner,‡ Taro Saito,* Akiko Asada,* Hiroyuki Kawahara,§ Nobuhisa Iwata,† Takaomi C. Saido† and Shin-ichi Hisanaga*

*Laboratory of Molecular Neuroscience, Department of Biological Sciences, Graduate School of Science and Engineering, Tokyo Metropolitan University, Hachioji, Tokyo, Japan

†Laboratory of Cell Biochemistry, Department of Biological Sciences, Graduate School of Science and Engineering, Tokyo Metropolitan University, Hachioji, Tokyo, Japan

‡Laboratory for Proteolytic Neuroscience, RIKEN BSI, Wako, Saitama, Japan

§Wolfson Institute for Biomedical Research, University College London, London, UK

Abstract

Cyclin-dependent kinase 5 (Cdk5) is a Ser/Thr kinase that is activated by binding to its regulatory subunit, p35. The calpain-mediated cleavage of p35 to p25 and the resulting aberrant activity and neurotoxicity of Cdk5 have been implicated in neurological disorders, such as Alzheimer's disease. To gain further insight into the molecular mechanisms underlying the pathological function of Cdk5, we investigated the role of the calpain inhibitor protein calpastatin (CAST), in controlling the aberrant production of p25. For this purpose, brain tissue from wild-type, CAST-over-expressing (transgenic), and CAST knockout mice were analyzed. Cleavage of p35 to p25 was increased in extracts from CAST knockout mice, compared with wild-type. Conversely, generation of p25 was not detected in brain lysates from CAST-over-expressing mice. CAST expression was 5-fold higher in mouse cerebellum than cerebral cortex. Accordingly, p25 production was lower in the cerebellum than the cerebral cortex. Furthermore, the Ca^{2+}-dependent degradation of p35 by proteasome was evident when calpain was inhibited. Taken together, these results suggest that CAST is a crucial regulator of calpain activity, the production of p25, and, hence, the deregulation of Cdk5. Therefore, impairment of CAST expression and its associated mechanisms may contribute to the pathogenesis of neurodegenerative disorders.

Keywords: Alzheimer's disease, calpain, calpastatin, cyclin-dependent kinase 5.

J. Neurochem. (2011) 117, 504–515.

Neurons are frequently exposed to physiological stimuli and pathological insults that increase intracellular Ca^{2+}. Physiologically, excitation allows the entry of Ca^{2+} into the pre-synaptic region to induce neurotransmitter release, and into the post-synaptic region to evoke signal transduction processes (Berridge 1998; Clapham 2007). In the pathological pathway involved in Alzheimer's disease (AD), accumulation of Aβ in neuronal plasma membranes impairs Ca^{2+} homeostasis (Hardy and Selkoe 2002). An increase in the levels of intracellular Ca^{2+}, regardless of whether this is a physiological or pathological event, activates a number of enzymes directly, or indirectly via Ca^{2+}-binding proteins. Calpain, a cytoplasmic Ca^{2+}-dependent cysteine protease, is one of the Ca^{2+}-activated enzymes (Saido et al. 1994; Goll et al. 2003; Suzuki et al. 2004). Although the physiological function of calpain in neurons has been suggested in synaptic

function and memory formation (Liu et al. 2008), the details of this mechanism remain unknown. In contrast, its patho-logical role is well documented, particularly during necrotic neuronal death (Bevers and Neumar 2008). Thus, the local or transient activation of calpain may promote its physiological

function (Liu *et al.* 2008), whereas excess activation of this protein is unfavorable for the survival of neurons.

The μ-calpain and m-calpain molecules are the major calpain forms expressed in neurons. These proteins become activated by Ca^{2+} concentrations in the μM and mM range, respectively (Saido *et al.* 1994; Goll *et al.* 2003; Suzuki *et al.* 2004). Both calpains are composed of an 80 kDa large catalytic subunit and a 30 kDa small regulatory subunit. These calpains are activated by autocleavage of the N-terminal inhibitory domain of the 80 kDa subunit, after conformational change upon the binding of Ca^{2+} (Strobl *et al.* 2000; Moldoveanu *et al.* 2002). Similarly, calpain usually cleaves substrate proteins at linker regions that connect globular functional domains, resulting in the alteration of their properties (Suzuki *et al.* 2004). As the activation of calpain is an irreversible reaction, calpain activation must be strictly controlled, particularly in neurons, which are vulnerable and exhibit limited regeneration. The inhibitory mechanism for calpain over-activation is critical, to avoid the undesired activation of calpain-dependent pathological pathways.

In addition to using the various mechanisms that maintain Ca^{2+} concentrations at a low level, cells also express a protein that inhibits calpain, calpastatin (CAST) (Murachi 1989; Goll *et al.* 2003). Full-length CAST is a 113 kDa protein including four tandem repeats of a calpain inhibitory domain that is composed of the so-called A to C sequences. Although CAST has been known for a long time (Murachi 1989), studies of its function, such as those using CAST transgenic (TG) or knockout (KO) mouse brains, are relatively recent. CAST-deficient mice show no apparent phenotype, but have high sensitivity to neurotoxic kainate (Takano *et al.* 2005). In contrast, a CAST TG mouse displays reduced cell death when neuronal toxicity is applied (Higuchi *et al.* 2005a; Rao *et al.* 2008). These results suggest a major role for CAST in pathological situations; however, the number of reports investigating the role of CAST in the development of AD remains limited (Vaisid *et al.* 2007; Rao *et al.* 2008; Liang *et al.* 2010).

Cyclin-dependent kinase 5 is a member of the Cdk serine/threonine kinase family, which is activated by the association with the regulatory subunit, p35 or p39. Cyclin-dependent kinase 5 (Cdk5) plays a role in a variety of neuronal activities, including neuronal migration, synaptic activity, and neuronal cell death (Ohshima *et al.* 1996; Dhavan and Tsai 2001; Lai and Ip 2009; Hisanaga and Endo 2010). p35 is a protein with a short half-life that is degraded by the ubiquitin–proteasome system in healthy neurons (Patrick *et al.* 1998; Saito *et al.* 1998). However, under pathological conditions of cell stress or injury, p35 can be cleaved by calpain to p25, which is a more stable fragment of p35 (Patrick *et al.* 1999; Kusakawa *et al.* 2000; Lee *et al.* 2000). The resulting Cdk5-p25 complex engenders aberrant activity and phosphorylates a number of substrates abnormally,

including the tau protein, which is a major component of paired helical filaments in AD. Aberrant phosphorylation of particular substrates is thought to induce neuronal cell death, leading to neurodegenerative diseases (Hisanaga and Endo 2010). Thus, the elucidation of the cleavage mechanism of p35 is critical for understanding the neuronal cell death caused by hyperactivated Cdk5. Here, we investigated the role of CAST in the cleavage of p35 to p25 using *CAST*-engineered animals and mouse brain regions exhibiting different CAST expression levels. The results suggest that CAST and Ca^{2+} are critical factors in the induction of p25-dependent Cdk5 hyperactivation in pathological conditions.

Materials and methods

Chemicals and antibodies

The anti-human CAST (H-300), anti-Cdk5 (DC17), and anti-p35 (C19) antibodies were purchased from Santa Cruz Biotechnology (Santa Cruz, CA, USA). The anti-spectrin (MAB1622) antibody was obtained from Calbiochem (San Diego, CA, USA). The anti-actin and anti-calpain 1 (μ-calpain) (2H2A7C2) antibodies were from Sigma (St Louis, MO, USA). The anti-calpain 2 (m-calpain) (AB81013) antibody was purchased from Chemicon (Temecula, CA, USA). Horseradish peroxidase-conjugated anti-rabbit or anti-mouse IgG was obtained from Dako (Glostrup, Denmark). The anti-mouse CAST antibody was described previously (Higuchi *et al.* 2005a; Takano *et al.* 2005), as was the PHF-1 aberrantly phosphorylated tau antibody (Otvos *et al.* 1994). Benzyloxycarbonyl-leucyl-leucyl-leucinal (MG132) and $A\beta_{1-42}$ were purchased from Peptide Institute (Osaka, Japan). Ionomycin, N-acetyl-leucyl-leucyl-norleucinal (ALLN), epoxomicin and the CAST peptide were obtained from Calbiochem. Puromycin, chloroquine diphosphate salt, and protease inhibitor cocktail were purchased from Sigma. z-VAD-FMK was obtained from Enzo Life Sciences International (Plymouth Meeting, PA, USA). Sodium pentobarbital (somnopentyl) was from Kyoritsu Seiyaku Corp. (Tokyo, Japan).

Preparation of recombinant CAST

Recombinant CAST was expressed in, and purified from, *Escherichia coli* (Maki and Hitomi 2000). Recombinant CAST bound to Ni-beads was eluted from the column using 50 mM sodium phosphate buffer, pH 7.5 containing 300 mM NaCl and 150 mM imidazole, and was dialyzed against HEPES buffer before use.

Animals

All animal experiments were performed according to the guidelines for animal experimentation of the Tokyo Metropolitan University. The mice were housed in cages of two to five littermates with access to food and water *ad libitum* in an environment subjected to a 12 h light/dark cycle. CAST TG or KO mice were bred as described previously (Higuchi *et al.* 2005a; Takano *et al.* 2005). ICR mice were obtained from Sankyo Laboratory Service (Tokyo, Japan). Mice were anesthetized with diethyl ether and perfused from the left ventricle using phosphate-buffered saline containing 1 mM EDTA. In some experiments, mice were decapitated without phosphate-buffered saline perfusion after anesthetization with diethyl ether.

Preparation of brain lysates and brain extracts

Lysates were prepared from snap-frozen human brain tissues from AD patients (four subjects, average age, 68 years (range, 60–76 years); average postmortem delay, 12.25 h (range, 9–18 h); two males and two females; all cases were Braak stage 5 or higher) and controls [three subjects, average age, 82.6 years (range, 76–87 years); average postmortem delay, 8.16 h (range, 6–11 h); three males] at the UCL Queen Square Brain Bank. In brief, small frozen tissue samples were homogenized in ice-cold P2 buffer containing protease and phosphatase inhibitors as described previously (Plattner et al. 2006). Mouse brains were dissected and homogenized in 10 volumes (volume/weight) of HEPES buffer (20 mM HEPES, pH 7.5, 5 mM KCl, 2 mM MgCl$_2$, 1 mM EGTA, and 1 mM dithiothreitol) at 4°C using a teflon pestle in a glass homogenizer.

p35 cleavage experiments

For in vitro. p35 cleavage experiments, the homogenates were centrifuged at 18 000 g for 20 min and the supernatants were used as brain extracts. The cleavage of p35 to p25 was induced by incubation of the brain extracts with the indicated concentrations of Ca^{2+} at 35°C. In some experiments, the incubation was carried out at 30°C to reduce the cleavage rate. Ca^{2+} concentrations were calculated using the Maxchelator software (http://maxchelator.stanford.edu/). In vitro degradation of p35 in the absence of Ca^{2+} was induced by incubation of the embryonic day 16 fetal brain extract with 10 µM microcystin and 1 mM ATP at 35°C for 1 and 3 h (Saito et al. 2003).

Neuronal cell cultures

The preparation and maintenance of primary cortical neurons were described previously (Minegishi et al. 2010). Cerebellar granule cells were cultured at a density of 4 × 10^6 cells/cm^2 in Neurobasal (Invitrogen, Carlsbad, CA, USA) medium. For the cleavage of p35 to p25 in neurons, primary neurons were treated with 10 µM or 20 µM ionomycin for 15 min at days in vitro 7 (DIV7) or 14 (DIV14). Primary cortical and cerebellar granule neurons at DIV14 were treated with 10 µM Aβ for 12 h. Neurotoxic Aβ aggregates were made by incubation at 37°C for 48 h in 10% (v/v) 60 mM NaOH and 90% (v/v) 10 mM phosphate buffer, pH 7.4 (Ono et al. 2010).

Global ischemia and reperfusion

Induction of ischemia–reperfusion was performed according to the method described previously (Uchino et al. 2002). Eight-week-old ICR mice were anesthetized with 50 mg/kg of sodium pentobarbital. Ischemia was induced by bilateral common carotid occlusion. After 5 min of ischemia, reperfusion of blood was restored for 30 min and brain extracts were prepared as described above.

Immunoprecipitation and Cdk5 activity assay

Cyclin-dependent kinase 5-p35 was immunoprecipitated from mouse brain extracts with anti-Cdk5 antibody C8 as described previously (Saito et al. 2003). The kinase activity of immunoprecipitated Cdk5-p35 was measured with 0.1 mM [γ-^{32}P]ATP and histone H1 as substrate at 37°C. Histone H1 phosphorylation was detected by autoradiography after sodium dodecyl sulfate–polyacrylamide gel electrophoresis and quantified with a liquid scintillation counter.

Sodium dodecyl sulfate–polyacrylamide gel electrophoresis and immunoblotting

Sodium dodecyl sulfate–polyacrylamide gel electrophoresis was performed using 12.5% acrylamide for p35 and Cdk5, 10% acrylamide for calpain and CAST, and 7.5% acrylamide for spectrin. Immunoblotting was performed as described previously (Sato et al. 2007).

Statistical evaluation

All of the experiments were performed a minimum of three times with similar results; representative results are shown. The statistical significance of the data was tested using Student's t-test to compare the two conditions. Differences were considered to be significant at $p < 0.05$ (*) or $p < 0.01$ (**).

Results

CAST levels in AD brains

Aberrant Cdk5 activity and increased levels of p25 have been implicated in neurodegenerative disorders, suggesting that in response to loss of Ca^{2+} homeostasis, calpain activation and hence the cleavage of p35 to p25 may contribute to the etiology of such diseases (Lee et al. 2000; Cruz and Tsai 2004). To test this hypothesis, we examined first the levels of CAST, an endogenous calpain inhibitor protein, in AD and control brains by immunoblotting using an anti-CAST antibody. AD pathology was confirmed by reaction with the PHF-1 antibody (Fig. 1a, middle panel), which recognizes phosphorylated tau protein (serine 396 and 404) and is commonly used as a marker of AD pathology (Otvos et al. 1994). As predicted, high levels of phospho-tau were selectively detected in the AD samples with no signal apparent in the corresponding controls. Interestingly, when the same samples were analyzed for CAST, a significant decrease in the endogenous calpain inhibitor was evident. The major band of CAST was detected at ~ 110 kDa, corresponding to the full length of human CAST (Fig. 1a,. upper panel). AD brain samples contained approx. 40% less CAST in comparison to control brains. A similar decrease was observed for a CAST fragment at 70 kDa (data not shown). These data indicate that CAST levels are reduced in AD.

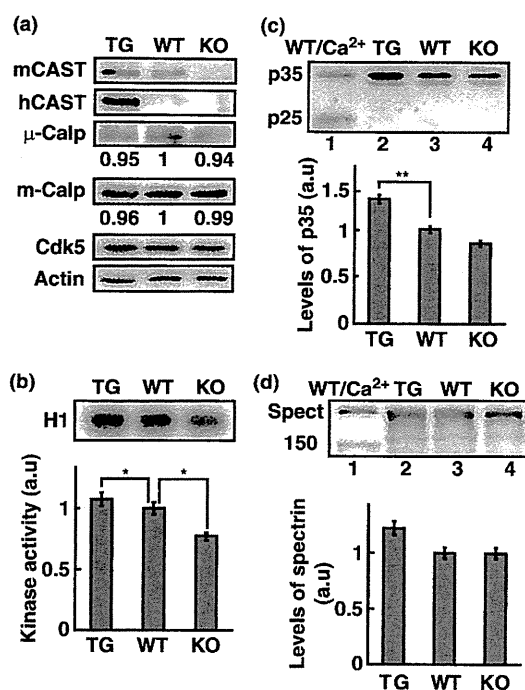## p35 cleavage to p25 in CAST transgenic or KO mouse brain extracts

It is possible that the reduced level of CAST in AD brains facilitates the hyperactivation of Cdk5 by calpain-mediated cleavage of p35 to p25. However, postmortem delay is inevitable in the case of human brains. Activation of calpain following death makes it difficult to estimate the pathological component of p25 production (Taniguchi et al. 2001). Given that levels of CAST inversely correlated with AD pathology, we went on to define the relationship between CAST, calpain, and p35 cleavage in genetically-modified animal

(a)

C1 C2 C3 A1 A2 A3 A4

CAST

pTau

Tub

(b)
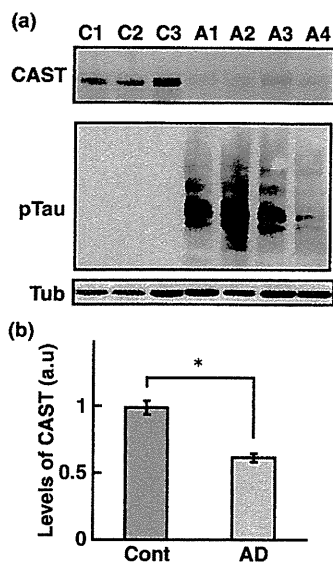
Fig. 1 Levels of the CAST protein in AD patients and controls. (a) Immunoblots of CAST in cortical/hippocampal lysates from healthy controls (C1–3) vs. AD patients (A1–4) (upper panel). Full-length CAST was detected at 113 kDa. Immunoblot detection of phosphorylated tau (pTau, middle panel) is also shown along with a loading control β-tubulin (Tub, lower panel). Phosphorylated Tau was probed with PHF-1 for tau pathology in AD brains, and tubulin was a loading control. Quantitation of levels of CAST detected in (a) is shown in (b). The levels of CAST in AD brains were 62 ± 0.2% of control brains (means ± SE; n = 3 for control and n = 4 for AD; *p < 0.05, Student's t-test).

models with altered CAST levels. We analyzed a TG mouse that over-expressed the human CAST gene under the control of the calcium-calmodulin kinase II (CaMKII) promoter. This model was compared to a constitutive CAST KO mouse as well as wild-type (WT) animals. Equal levels of expression of mouse CAST were detected in TG and WT mouse whole brain lysates, while none was present in the CAST KO (Fig. 2a, top panel). In contrast, human CAST was detected only in TG brain (Fig. 2a, second panel). There was no discernible affect on the expression of µ-calpain, m-calpain, Cdk5, or actin. The effect of these changes in CAST expression on Cdk5 activity was next examined. A Cdk5 immunoprecipitation kinase activity assay using Histone H1 as a substrate showed that Cdk5 activity is marginally increased in TG brains (107%) and decreased in KO brain (77%) compared with WT brain (Fig. 2b).

Next, we investigated the levels of p35 and p25. It should be noted that p25 represents a truncated form of p35, in which the first 100 N-terminal amino acids are removed by calpain-dependent cleavage. Thus, an antibody specific for the C-terminus can be used to detect both p35 and p25 by immunoblotting. To control for this, acutely prepared WT mouse brain lysate was incubated in 1 mM Ca^{2+} for 30 min.

(a)

	TG	WT	KO
mCAST			
hCAST			
µ-Calp			
	0.95	1	0.94
m-Calp			
	0.96	1	0.99
Cdk5			
Actin			

(c) WT/Ca²⁺ TG WT KO

p35

p25

1 2 3 4

(b) TG WT KO

H1

(d) WT/Ca²⁺ TG WT KO

Spect

150

1 2 3 4

Fig. 2 The effect of transgenic over-expression or knockout of CAST on levels of p35 and Cdk5 activity. (a) Immunoblots of mouse CAST (mCAST), human CAST (hCAST), µ-calpain (µ-calp), m-calpain (m-calp), Cdk5, and actin in TG, KO, or WT mouse brain. Relative ratios of the expression of µ- and m-calpain are indicated below the respective blots, 0.95 ± 0.07 and 0.94 ± 0.06 for m-calpain in TG and KO mice, and 0.96 ± 0.03 and 0.99 ± 0.01 for m-calpain in TG and KO mice (means ± SE; n = 3; *p < 0.05, Student's t-test). (b) The kinase activity of Cdk5 in TG, KO, or WT mouse brain. The kinase activity was measured with Cdk5-p35 immunoprecipitated from brain extracts of 1-year-old TG, KO, or WT mice using histone H1 as a substrate (upper panel). Quantification is shown in lower panel. Bars indicate the means ± SE (n = 3; *p < 0.05, Student's t-test). (c) and (d) Immunoblots of p35 and spectrin (Spect) in TG, KO, or WT mouse brain. The 25 kDa cleavage product of p35 (p25) and the 150 kDa cleavage product of spectrin were detected in lane 1 (WT/Ca²⁺), in which the samples were derived by incubating the WT mouse brain extract with 1 mM Ca^{2+} for 30 min at 37°C. Quantification of p35 and spectrin in CAST TG, KO, and WT mouse brains is shown in lower panels of (c) and (d). Bars indicate the means ± SE (n = 3; *p < 0.05 and **p < 0.01, Student's t-test).

Consistently, this treatment resulted in p25 production (Fig. 2c, lane 1). However, no p25 was detected in the brain extracts acutely prepared from any of TG, KO and WT mice. Interestingly, TG mice exhibited a 1.35-fold increase in p35 in comparison to WT. Furthermore, KO mice displayed a reduction in p35 levels to 85.2% of that detected in WT controls, though the reduction was not statistically significant. To gain further insight a second analysis was conducted using a well-defined calpain substrate, spectrin, which is a

cytoskeletal scaffolding protein that complexes with actin. Similar to p35, addition of Ca^{2+} to a brain extract induces cleavage of the full-length protein to the 150 kDa calpain-cleavage product (Fig. 2d, lane 1). In contrast to p35, levels of spectrin were not appreciably affected by changes in CAST expression. On the other hand, as with p25, no calpain-cleaved product of spectrin was produced in these mice under basal conditions. These data indicate that p35 levels inversely correlate with CAST levels and raise the possibility that mechanisms beside calpain cleavage may contribute to p35 expression.

Given very little p25 is detected in normal healthy mouse brains, it is not surprising that in the absence of stress or pathology, no p25 was detected even in the absence of CAST expression. To better understand how factors such as loss of Ca^{2+} homeostasis could affect p35 and p25 levels a simple model was used in which acutely prepared whole brain extracts were treated with various times or amounts of Ca^{2+} to invoke Ca^{2+} dependent molecular mechanisms. A treatment of extracts from TG, WT, or KO mice for 0, 10 or 60 min revealed interesting differences in p35 degradation as a result of changes in CAST expression (Fig. 3a). Specifi-

cally, this treatment resulted in time-dependent reduction in p35 levels. However, the rate of this reduction was apparently increased in the KO mice lacking CAST expression. Furthermore, as p35 levels were reduced, no p25 was generated in the CAST TG mouse. However, p25 was prominently detected in response to Ca^{2+} at the 10 min time point of incubation in the WT and KO mouse brain extracts. Cdk5 levels were unaffected by any of these treatments. The pattern for degradation of spectrin was similar to p35, although the 150 kDa calpain cleavage product was produced in all mice including the CAST TG line. These data further point to some specificity in the ability of CAST to protect p35 from calpain-dependent cleavage.

To more carefully characterize the kinetics of conversion of p35 to p25 in WT vs. CAST KO mice, a more careful time course was conducted at 30°C (Fig. 3b). Quantification of p25 production is shown in Fig. 3(c). In this format, it was more apparent that the initial production of p25 occurred earlier and in a more pronounced manner in KO compared with WT mouse brain extracts (Fig. 3b and c). Taken together, these data show that CAST expression regulates the calpain-dependent cleavage of p35 to p25, while pointing to
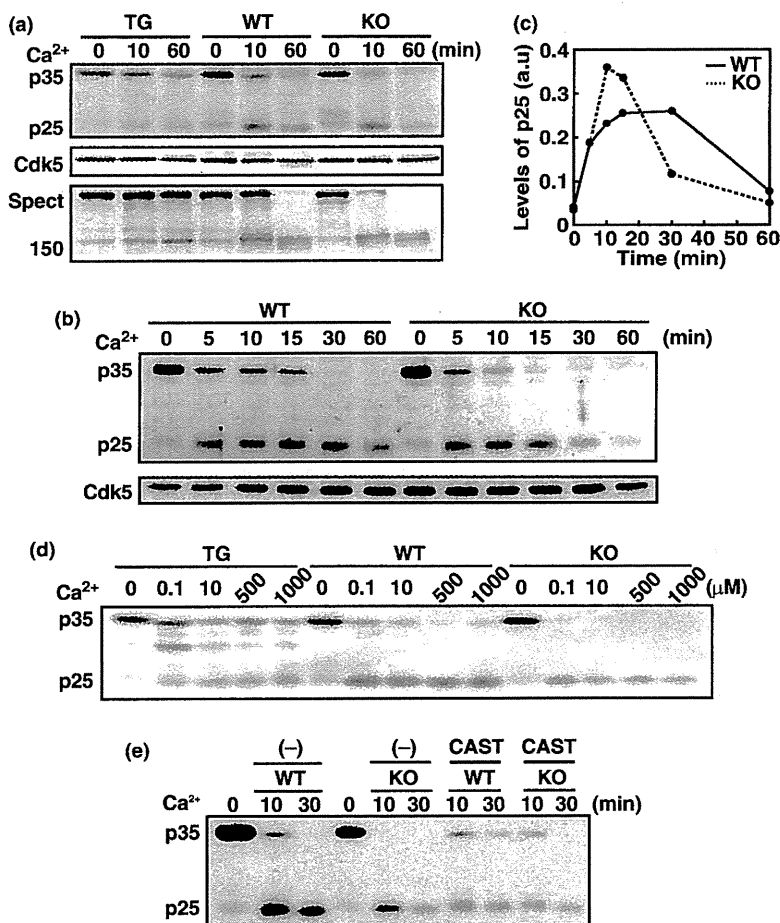
Fig. 3 Cleavage of p35 by calpain in CAST TG or KO mouse brain extracts. (a) Immunoblots show the effect of treatment of CAST TG, KO, or WT mouse brain extracts with 1 mM Ca^{2+} for the indicated period of time. Immunoblots for p35/p25, Cdk5, and spectrin are shown. (b) Characterization of the effects of 2 mM Ca^{2+} on p35 degradation and p25 production in CAST KO vs. WT mouse brain extracts over the broader timecourse indicated. Incubation with Ca^{2+} was carried out at 30°C in this experiment. An immunoblot of Cdk5 is also shown. This is a typical result from three independent experiments. Quantification of p25 production is normalized with Cdk5 and shown in (c). (d) Comparison of 35 cleavage in extracts from CAST TG, KO, or WT mouse brains with treatments over a range of Ca^{2+} concentrations. (e) Cleavage of p35 to p25 in WT vs. CAST KO mouse brain extracts with 1 mM Ca^{2+} in the absence (−), or presence of additional recombinant CAST.

the possibility that in the absence of calpain activity, p35 levels are regulated by some other Ca^{2+}-dependent mechanism.

In addition to kinetics, the dose-response relationship between Ca^{2+} and p35/p25 levels was evaluated by treating brain extracts with various concentrations of Ca^{2+} (Fig. 3d). Using this approach, p35 levels were reduced in TG mouse brain extracts, as was observed in the time-course experiment, even when incubated with only 0.1 μM Ca^{2+}. As in the time-course experiments, both WT and KO mouse extracts produced p25 in response to all levels of Ca^{2+}. However, some p35 remained in WT mice at 0.1 μM Ca^{2+} while only p25 was appreciated in the KO mice. Furthermore, less p25 was detected, even in the absence of any remaining p35 in the KO mouse brain extracts possibly because of further Ca^{2+}-depedent degradation subsequent to calpain-dependent generation of p25.

To ensure that these effects were because of changes in the levels of the CAST protein, and not to the secondary consequences of other changes induced by CAST transgenesis and knockout, we performed rescue experiments, in which the WT and KO mouse brain extracts were complemented with recombinant purified CAST. Supplementation of the WT and KO mice brain extracts with 150 nM recombinant CAST attenuated Ca^{2+}-dependent generation of p25, but had no effect on the disappearance of p35 (Fig. 3e, CAST). The effect of CAST at different concentrations (from 5 nM to 350 nM) was also examined in the WT and KO mouse brain extracts (Figure S1). The inhibition of p25 generation by exogenous CAST was concentration-dependent. These results suggest that CAST regulates the cleavage of p35 to p25 in brains.

Differential expression of CAST and differential cleavage to p25 between cerebral cortex and cerebellum

Calpastatin TG and KO mice are extreme cases, as the amounts of CAST are genetically modulated in these animals. Therefore, we wanted to assess the effect of CAST on the production of p25 in WT animals. It was reported recently that CAST levels are different in the cerebrum and in the cerebellum (Vaisid et al. 2007). We thought that this could represent a natural model to investigate the effect of CAST on p25 production. First, we examined the levels of CAST in several brain regions, i.e., the cerebral cortex, cerebellum, hippocampus, striatum, and olfactory bulb, using immunoblotting with anti-CAST and anti-p35 antibodies. As reported previously, the levels of CAST were about 5-fold higher in the cerebellum compared with the cerebral cortex (Fig. 4a and b). Expression of CAST was low in the hippocampus ($\sim$ 60% of that observed in the cerebral cortex), but its expression in the striatum and olfactory bulb was about two times higher compared with that observed in the cerebral cortex. In contrast, we found that the amount of p35 was lower in the cerebellum than it was in the other brain

regions. Consistent with the reduced protein amount of p35, the Cdk5 activity in the cerebellum was decreased by approx. 33% as compared to cortex (Fig. 4c). Although the expression of m-calpain was slightly lower in the cerebellum ($\sim$ 90% of that detected in the cerebral cortex), the levels of Cdk5 and μ-calpain were about 1.5 times higher in the cerebellum compared with the cerebral cortex.

We compared the production of p25 between the cerebral cortex and the cerebellum. Cortical or cerebellar extracts were incubated with 1 mM Ca^{2+} for the indicated times and cleavage was examined by immunoblotting using an anti-p35 antibody (Fig. 4d). In the blot of Fig. 4(d), the amount of p35 was adjusted to allow the easy comparison of the production of p25 between the two brain regions. The decrease in p35 and increase in p25 were quantified in both extracts (Fig. 4e). The amount of p35 was reduced slightly faster in cerebellar extracts (Fig. 4e, solid line of right panel) compared with cortical extracts (Fig. 4e, solid line of left panel). p25 production was higher in cortical extracts compared with cerebellar extracts (Fig. 4d and e); in addition, the p25 generated in cerebellar extracts was decreased after longer incubation (Fig. 4e, dotted line of right panel). Therefore, the total amounts of p35 and p25 were reduced in cerebellar extracts after incubation, whereas those detected in cortical extracts were roughly constant.

Next, we examined the effect of CAST on the production of p25 in cellular conditions using primary neurons prepared from cerebral cortex or cerebellum. The amount of CAST was about 2-fold higher in cerebellar granule cells than it was in cerebral cortical neurons (Fig. 5a). The cleavage of p35 was induced by treatment of neurons with the calcium ionophore ionomycin for 15 min. The amount of p35 at time 0 was adjusted to make the comparison of p25 production easy. A strong signal for p25 was detected in cerebral cortical neurons, but p25 was not increased in cerebellar granule cells (Fig. 5b). The levels of CAST increased from DIV4 to DIV14 of the cultivation of cerebellar granule cells (Fig. 5c). The cleavage of p35 to p25 was compared in cerebellar granule cells between DIV7 and DIV14. The amount of p25 increased significantly in cerebellar granule cells at DIV7, but not at DIV14, after ionomycin treatment (Fig. 5d). To evaluate the effect of CAST to molecular mechanisms underlying AD, we treated cultured cortical or cerebellar neurons with Aβ and examined the p25 production. While p25 was detected in cortical neurons treated with Aβ, the same treatment failed to generate p25 in cerebellar granule neurons (Fig. 5e). These results also indicate that the levels of CAST regulate the calpain-mediated generation of p25 in neurons.

The cleavage of p35 was investigated further at the individual level using postmortem and ischemic mouse brains. The production of p25 was compared between the cerebral cortex and the cerebellum of mice kept at 25°C after killing by cervical dislocation. Although p25 was generated
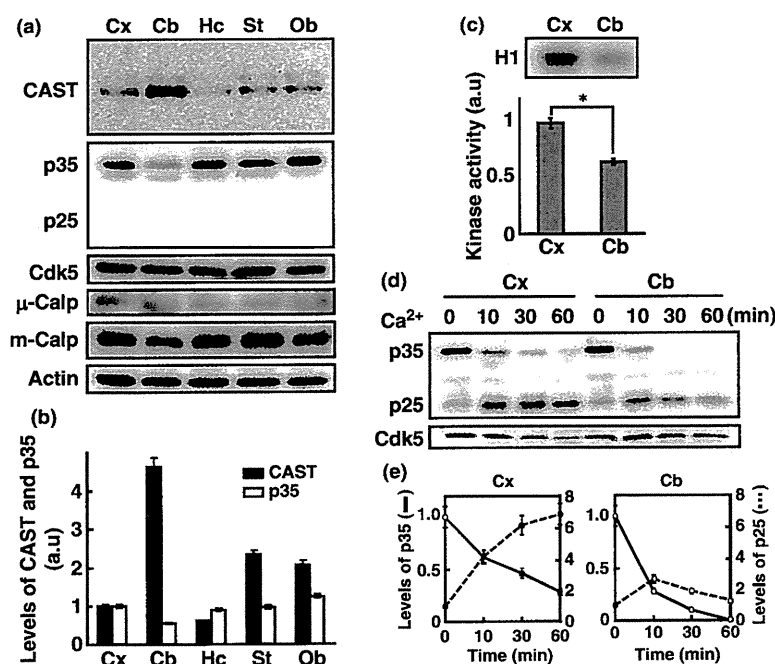
Fig. 4 Regional distribution of CAST in mouse brain and the p35 cleavage in cerebral cortex and cerebellum. (a) Immunoblots of lysates from adult mouse cerebral cortex (Cx), cerebellum (Cb), hippocampus (Hc), striatum (St), and olfactory bulb (Ob) for CAST, p35, Cdk5, μ-calpain, m-calpain, and actin. (b) Ratio of the expression of p35 and CAST in the various brain regions relative to their expression in the cerebral cortex. Bars indicate the means ± SE (n = 3; *p < 0.05, Student's t-test). Black bar is CAST and white bar is p35. (c) The kinase activity of Cdk5-p35 in mouse cerebral cortex and cerebellum. The kinase activity was measured as described in the legend of

Fig. 2(b). The Cdk5 activity in cerebellum was 64 ± 4% of that of cortex (means ± SE; n = 3; *p < 0.05, Student's t-test). (d) Comparison of the cleavage of p35 to p25 in extracts from cerebral cortex vs. cerebellum. The extracts were treated with 1 mM of Ca^{2+} for the indicated period. Immunoblots of p35/p25 and Cdk5 are shown. (e) Quantification of p35 and p25 in the cerebral cortex (Cx, left panel) and cerebellum (Cb, right panel). The levels of p35 (solid lines) are indicated by the scale of left side vertical axis and those of p25 are by the scale of right side vertical axis. Bars indicate the means ± SE (n = 3; *p < 0.05, Student's t-test).

in both the cerebral cortex and cerebellum after 30 min of postmortem delay, more p25 was detected in the cerebral cortex compared with the cerebellum (Figure S2). p25 accumulated gradually in the cerebral cortex with increasing time of postmortem delay, up to 3 h, whereas the levels of p25 decreased slightly in the cerebellum after 1 h of postmortem delay, in spite of the significant decrease in the levels of p35. To examine the generation of p25 under controlled *in vivo* experimental conditions, we used an ischemia–reperfusion system, which activates calpain in the brain (Yokota *et al.* 1995). Global ischemia was induced by 5 min of bilateral common carotid occlusion, which was followed by 30 min of reperfusion (Uchino *et al.* 2002). The production of p25 was compared between the cerebral cortex and the cerebellum by immunoblotting using an anti-p35 antibody (Fig. 6a). The levels of p25 generated in the cerebellum is expressed as the relative ratio to that in the cerebral cortex after normalizing the p35 levels between control cortex and cerebellum (Fig. 6b). The generation of p25 was higher in the cerebral cortex than in the cerebellum.

These results indicate that CAST regulates the calpain-mediated cleavage of p35 to p25 *in vivo* in brains.

**Calcium-dependent proteasomal degradation of p35**

As was shown above, the calcium-induced degradation of p35 was observed in CAST TG mouse brain extracts (Fig. 3a) and in cerebellar extracts (Fig. 4d). To identify the protease involved in this degradation of p35, we incubated TG mouse brain extracts with 1 mM Ca^{2+} in the presence of various protease inhibitors, such as ALLN (calpain inhibitor), z-VAD (caspase inhibitor), chloroquine (cathepsin D inhibitor), puromycin (aminopeptidase A inhibitor), and MG132 (proteasome inhibitor) (Fig. 7a). MG132 alone inhibited the degradation of p35. These results indicate that the calcium-induced degradation of p35 is catalyzed by the proteasome.

Although, we have previously investigated the proteasomal degradation of p35 (Saito *et al.* 1998; Wei *et al.* 2005; Minegishi *et al.* 2010), its mechanism is not yet completely resolved. The calcium dependence of p35 degradation
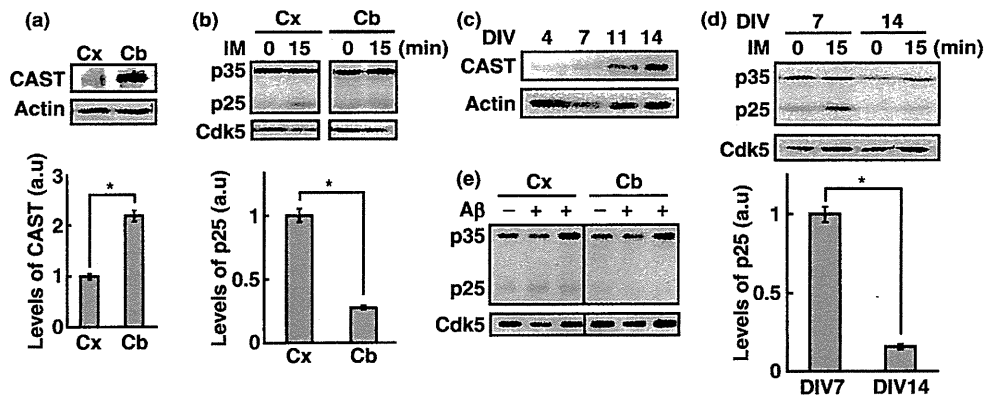
Fig. 5 Cleavage of p35 to p25 in cultured cortical or cerebellar neurons. (a) Immunoblots of extracts from mouse primary cultured cortical (Cx) and cerebellar (Cb) neurons at DIV14 for CAST or actin. Quantification of CAST is shown in the lower panel. Bars indicate the means ± SE ($n = 3$; *$p < 0.05$, Student's paired t-test). (b) The effect of the Ca^{2+} ionophore, ionomycin (IM, 10 μM, 15 min) on p25 levels in Cx vs. Cb cultured neurons. Immunoblots for p35/p25 and Cdk5 are shown with quantitation of p25 levels (lower panel). Bars indicate the means ± SE ($n = 3$; *$p < 0.05$, Student's t-test). (c) The effect of time in culture on CAST expression in primary cultured cerebellar neurons.

Immunoblots of CAST and actin in lysates from cultures maintained for the indicated number of days in vitro (DIV) are shown. (d) The effect of ionomycin (IM, 20 μM, 15 min) on p25 levels in primary cerebellar neurons at DIV7 and DIV14. Immunoblots of p35/p25 and Cdk5 are shown with quantitation of p25 (lower panel). Bars indicate the means ± SE ($n = 3$; *$p < 0.05$, Student's t-test). (e) Aβ-induced p25 production in cortical or cerebellar neurons. Mouse cortical neurons (Cx) and cerebellar neurons (Cb) at DIV14 were treated with 10 μM Aβ$_{1-42}$ for 12 h (+). Immunoblots for p35/p25 and Cdk5 are shown in duplicate.
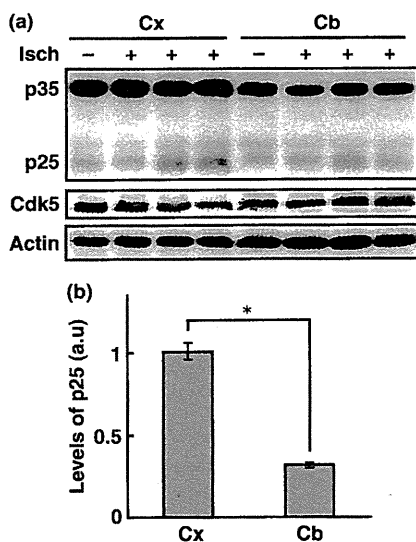
Fig. 6 Effects of ischemia on the cleavage of p35 to p25 in mouse cortex vs. cerebellum. (a) Ischemia induced p25 generation to different levels in Cx vs. Cb. Immunoblots of p35/p25, Cdk5, and actin are shown with quantitation (b). The p25 was measured and normalized to the amount of p35 in control mouse brain cortex or cerebellum. The production of p25 in the cerebellum is expressed as the relative ratio to that in the cerebral cortex after normalizing the p35 levels between cortex and cerebellum. Bars indicate the means ± SE ($n = 3$; *$p < 0.05$, Student's t-test).

became apparent here in the presence of an excess amount of CAST, which suppressed the activation of calpain. To determine whether the calcium-dependent proteasomal degradation of p35 occurs in WT mouse brains, we incubated WT brain extracts with 1 mM Ca^{2+} in the presence of the calpain inhibitor CAST peptide. Even when the cleavage to p25 was inhibited by the CAST peptide, the levels of p35 were still decreased after incubation with Ca^{2+} (Fig. 7b, lane 3). This decrease in p35 was prevented by the administration of MG132 (Fig. 7b, lane 4) or of the more specific proteasome inhibitor epoxomicin (Fig. 7b, lane 5). The same result was obtained using rat brain extracts (data not shown). We tested if CAST affects the degradation of p35 in the absence of Ca^{2+} using the in vitro degradation assay (Saito et al. 1998). p35 in fetal mouse brain extract was degraded by incubating with protein phosphatase inhibitor microcystin and ATP (Figure S3, lanes 2 and 3), but the addition of recombinant CAST did not change the degradation of p35 (Figure S3, lanes 4 and 5). These results suggest that CAST regulates only the Ca^{2+}-dependent degradation of p35.

We examined the calcium-dependent degradation of p35 further in primary cortical neurons. Treatment of mouse brain cortical neurons with low (5 μM) or high (20 μM) concentrations of ionomycin for 60 min led to the generation of the p25, which was inhibited by ALLN, in the presence of 20 μM ionomycin (Fig. 7c, lane 5); in contrast, 5 μM ionomycin induced the degradation of p35 without the production of p25 (Fig. 7c, lane 2). This decrease was
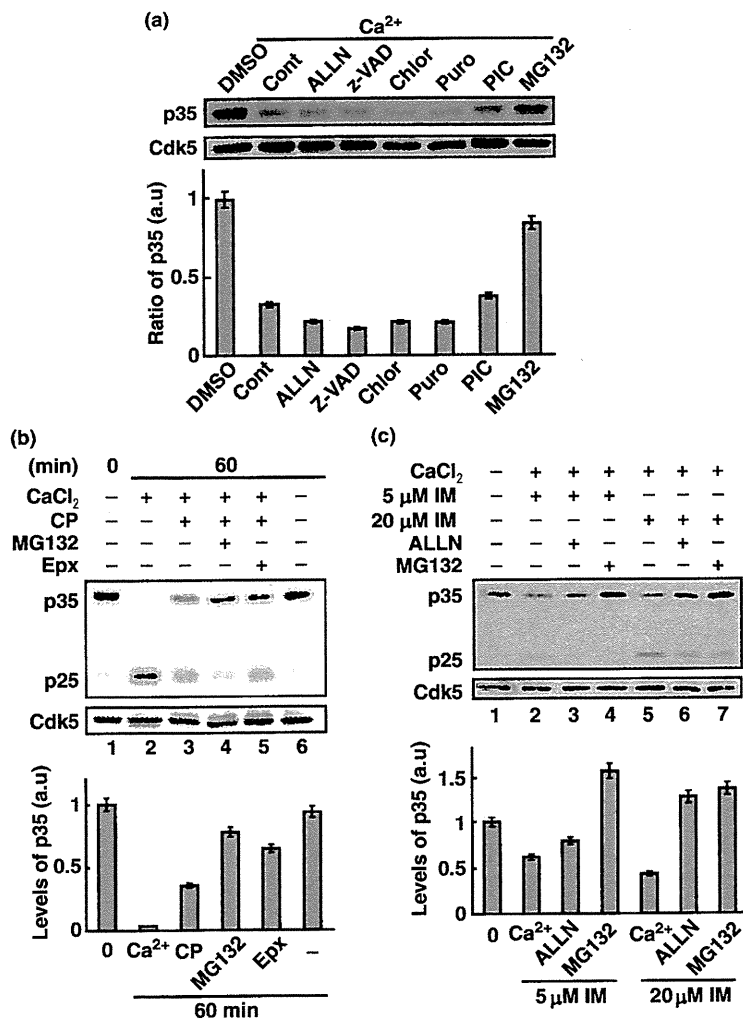
Fig. 7 The pathway of p35 degradation is determined by CAST. (a) The effects of various protease inhibitors on p35 degradation in CAST TG mouse brain extracts treated with 1 mM Ca^{2+}. Lysates were incubated with vehicle (DMSO), non (Cont), or treated with an inhibitor of calpain (ALLN, 10 μM), caspase (z-VAD, 1 mM), cathepsin D (Chlor, chloroquine, 100 μM), aminopeptidase (Puro, puromycine, 1 mM), a protease inhibitor cocktail (PIC containing AEBSF, aprotinin, leupeptin, bestatin, pepstatin A, and E-64), or a proteasome inhibitor (MG132, 10 μM). Immunoblots of p35 and Cdk5 are shown, with quantitation for p35 (means ± SE; n = 3). (b) CAST switches p35 from calpain-dependent cleavage to proteasome-dependent degradation. The effect of 1 mM Ca^{2+} on mouse brain extract p35/p25 levels in the presence of CAST peptide (CP), MG132, or the proteasome inhibitor epoxomicin (Epx) is shown in immunoblots, with quantitation of p35 (means ± SE; n = 3). (c) The level of Ca^{2+} ionophore determines the pathway of p35 degradation. The effect of 5 vs. 20 μM ionomycin (IM) in the presence of 2 mM Ca^{2+} in the presence of either the calpain inhibitor ALLN or the proteasome inhibitor MG132 is shown in immunoblots of p35/p25 and Cdk5, with quantitation of p35 levels (means ± SE; n = 3).

inhibited by MG132, but not by ALLN (Fig. 7c, lanes 3 and 4). These results indicate that p35 is degraded by the proteasome in neurons in a calcium-dependent manner.

Discussion

Here, we investigated the role of CAST in the cleavage of the p35 Cdk5 activator to p25. For this purpose, we performed a differential analysis of CAST TG, CAST KO and WT mouse brain extracts, from cerebral cortex and cerebellum. In all experimental paradigms, the increased levels of CAST abrogated the cleavage of p35 to p25. Thus, it is conceivable that the decreased CAST levels in AD brains could lead to calpain-dependent hyperactivation of Cdk5 thereby contributing to the pathogenesis of AD. Furthermore, we found that p35 was degraded by the proteasome in a calcium-dependent manner. Thus, the calcium-dependent regulation of the CAST–calpain and ubiquitin–proteasome systems seems to play a pivotal role in the regulation of the Cdk5 activity in the brain.

It is well documented that calpain is activated during neuronal cell death through various insults, such as ischemia and glutamate or kainate cytotoxicity (Saido *et al.* 1994; Xu *et al.* 2007; Liu *et al.* 2008). Activated calpain cleaves many proteins, leading to exacerbation of the cellular death processes. However, it has not been determined conclusively whether calpain activation is a primary cause of this phenomenon. In contrast, it has been proposed that calpain activation is a result of neuronal death under conditions in which neurons cannot maintain the intracellular calcium concentration at a low level. We examined here the role of CAST in calpain activation *in vitro* and *in vivo*. For this purpose, we used two different mouse models, which exhibit opposing changes in CAST levels, namely the CAST TG and CAST KO mice. Calpain activation occurred easily in brain tissue from KO mice, as well as in tissue from brain regions,

such as the cerebellum, that express low levels of CAST. At low levels of CAST, calpain was activated concomitantly with the small and transient increase in Ca^{2+} that is insufficient to activate calpain under normal conditions. These results implicate the possibility that calpain overactivation is a cause of neuronal cell death, if the levels of CAST are low or reduced.

Calpastatin was decreased significantly in AD (Rao et al. 2008 and this study). These results suggest that neurons in AD brains cannot regulate the level of activation of calpain, even when a subtle insult is applied. Many reports have demonstrated hyperactivation of Cdk5 by the calpain-mediated cleavage of p35 to p25 in neurodegenerative diseases, including AD (Patrick et al. 1999; Lee et al. 2000; Cruz and Tsai 2004). Consistently, p25-induced Cdk5 activation can indirectly mediate abnormal tau phosphorylation via deregulation of glycogen synthase kinase 3 (GSK3) (Plattner et al. 2006). In addition, recent reports suggest a possible involvement of the calpain–Cdk5 cascade in AD neurodegeneration through beta-secretase (BACE)-Aβ feedback loop (Zheng et al. 2005; Cruz et al. 2006; Wen et al. 2008; Liang et al. 2010). One of the remaining questions is, why the levels of CAST are decreased in AD brains. CAST is degraded mainly by calpain in adult brains (Higuchi et al. 2005a). Decreased expression of CAST in AD patients, in which massive neurodegeneration has already occurred, might be simply a result of calpain activation. Alternatively, CAST expression may be decreased in AD, over the age-dependent reduced expression (Averna et al. 2001) for unidentified reasons. Our finding of the easy induction of the hyperactivation of Cdk5 in the cerebral cortex with the low levels of CAST expression supports the latter possibility, i.e., that the reduced levels of CAST could be a cause of the initial activation of calpain. Activated calpain may downregulate CAST further. As a result of this kind of positive activation loop, calpain would attain an abnormally high activity in neurons, leading to neurodegeneration. If this is the case, the inhibition of calpain activation would be a likely candidate to achieve the prevention of AD, because the inhibition of calpain does not induce any apparent deleterious effects in healthy neurons (Higuchi et al. 2005b; Liu et al. 2008; Pietsch et al. 2010). Moreover, CAST is a promising candidate for inhibition of calpain overactivation in neurodegenerative diseases.

Calpastatin was identified as an inhibitor of calpain more than 20 years ago (Murachi 1989). No other function of CAST has been indicated (Goll et al. 2003). The physiological, as well as pathological, functions of CAST in the brain were challenged recently by the generation of CAST KO and TG mice (Higuchi et al. 2005a; Takano et al. 2005; Rao et al. 2008; Liang et al. 2010). The two types of mice, either over-expressing CAST or lacking CAST, respectively, exhibited no apparent phenotype in normal conditions. In contrast, in pathological conditions, neurons expressing more

CAST were resistant to a kainate insult (Higuchi et al. 2005a; Rao et al. 2008), whereas neurons deficient in CAST showed vulnerability to this insult (Takano et al. 2005). These results confirmed that CAST plays a major role in pathological neurodegeneration when calpain is activated. Later, behavior analysis of CAST KO mice found that these animals display a deficiency in the acoustic startle response and decreased locomotive activity in a stressful environment (Nakajima et al. 2008), suggesting the possibility that CAST also has a physiological function in synaptic activity. The question remains whether the deficiency in the acoustic startle response and the decreased locomotive activity are a result of calpain activation in stressful environmental conditions. If the function of CAST is associated exclusively with calpain inhibition, these results may mean that calpain participates in some of the affective motor activities. The report of a study using μ-calpain KO mice described a role for this protein in post-synaptic function (Grammer et al. 2005). If calpain is not involved in locomotive function, however, these results suggest a novel function of CAST that is independent of calpain. Several locomotive behaviors are controlled by cerebellar neurons, where CAST is expressed abundantly. Although the reason for the extremely high levels of expression of CAST in the cerebellum remains unknown, the high levels of CAST may be connected with cerebellar motor function. In any case, to date, there is no clear evidence indicating that stronger suppression of calpain activation by high CAST expression is deleterious in neurons.

The proteasome is a non-lysosomal protease system that degrades ubiquitinated proteins (Goldberg 2003; Tanaka 2009). The proteasome regulates a number of physiological cellular processes, including the cell cycle, immune response, endoplasmic reticulum stress response, and metabolism, in a manner that differs from that observed for calpain, which functions mainly in pathological cell death. Therefore, the proteasome has several properties that are in contrast to those of calpain. For example, the proteasome is active in normal cellular conditions, in which calpain is usually inactive. Nonetheless, the cross-talk between the ubiquitin–proteasome system and calpain has been suggested. For example, inhibition of the proteasome induces the calpain-mediated cleavage of IkappaB (IkB) (Li et al. 2010). Here, we used CAST TG and KO mice to show that the levels of the p35 protein increased in parallel with the increase in the expression of CAST. p35 is a protein that has a short half-life and is degraded by the proteasome. The increased amount of p35 suggests the decreased turnover rate of p35 in CAST TG mouse brains, although CAST did not affect the in vitro degradation of p35 in the absence of Ca^{2+}. It is not known how CAST regulates the proteasome-dependent p35 degradation.

Finally, we found the calcium-dependent degradation of p35 using CAST TG mouse brains, in which the calpain-

dependent cleavage of p35 to p25 was suppressed. This calcium-dependent degradation was also seen in WT brains in the presence of calpain inhibitors. The degradation of p35 was induced in neurons via treatment with glutamate or NMDA (Wei *et al.* 2005; Hosokawa *et al.* 2006). The NMDA-induced degradation of p35 was regulated by calcium (Wei *et al.* 2005); we thought that calcium may stimulate the activity of Cdk5 to phosphorylate p35, which represents a tag for ubiquitination. According to the present results, however, calcium seems to stimulate the ubiquitination or degradation of p35, rather than the activity of Cdk5-p35. It was proposed that the NMDA-dependent degradation of p35 is involved in synaptic plasticity (Wei *et al.* 2005). As described above, the involvement of CAST in synaptic activity was also suggested by the decreased locomotive activity observed in CAST KO mice (Nakajima *et al.* 2008); CAST may contribute to synaptic activity via the regulation of proteasome activity. CAST-engineered mice may represent animal models that will be useful for the more detailed investigation of the calcium-dependent degradation system.

Acknowledgements

Supporting information

Additional supporting information may be found in the online version of this article:

Figure S1. Dose-dependent inhibition of the cleavage of p35 to p25 by recombinant CAST.

Figure S2. Production of p25 in the cerebral cortex or cerebellum during postmortem delay.

Figure S3. Effect of CAST on *in vitro* p35 degradation in the absence of Ca^{2+}.

As a service to our authors and readers, this journal provides supporting information supplied by the authors. Such materials are peer-reviewed and may be re-organized for online delivery, but are not copy-edited or typeset. Technical support issues arising from supporting information (other than missing files) should be addressed to the authors.

References

Averna M., De Tullio R., Salamino F., Minafra R., Pontremoli S. and Melloni E. (2001) Age-dependent degradation of calpastatin in kidney of hypertensive rats. *J. Biol. Chem.* **276**, 38426–38432.

Berridge M. J. (1998) Neuronal calcium singnaling. *Neuron* **21**, 13–26.

Bevers M. B. and Neumar R. W. (2008) Mechanistic role of calpains in postischemic neurodegeneration. *J. Cereb. Blood Flow Metab.* **28**, 655–673.

Clapham D. E. (2007) Calcium signaling. *Cell* **131**, 1047–1058.

Cruz J. C. and Tsai L. H. (2004) Cdk5 deregulation in the pathogenesis of Alzheimer's disease. *Trends Mol. Med.* **10**, 452–458.

Cruz J. C., Kim D., Moy L. Y., Dobbin M. M., Sun X., Bronson R. T. and Tsai L. H. (2006) p25/cyclin-dependent kinase 5 induces production and intraneuronal accumulation of amyloid beta in vivo. *J. Neurosci.* **26**, 10536–10541.

Dhavan R. and Tsai L. H. (2001) A decade of CDK5. *Nat. Rev. Mol. Cell Biol.* **2**, 749–759.

Goldberg A. L. (2003) Protein degradation and protection against mis-folded or damaged proteins. *Nature* **426**, 895–899.

Goll D. E., Thompson V. F., Li H., Wei W. and Cong J. (2003) The Calpain system. *Physiol. Rev.* **83**, 731–801.

Grammer M., Kuchay S., Chishti A. and Baudry M. (2005) Lack of phenotype for LTP and fear conditioning learning in calpain 1 knock-out mice. *Neurobiol. Learn. Mem.* **84**, 222–227.

Hardy J. and Selkoe D. J. (2002) The amyloid hypothesis of Alzheimer's disease: progress and problems on the road to therapeutics. *Science* **297**, 353–356.

Higuchi M., Tomioka M., Takano J., Shirotani K., Iwata N., Masumoto H., Maki M., Itohara S. and Saido T. C. (2005a) Distinct mechanistic roles of calpain and caspase activation in neurodegeneration as revealed in mice overexpressing their specific inhibitors. *J. Biol. Chem.* **280**, 15229–15237.

Higuchi M., Iwata N. and Saido T. C. (2005b) Understanding molecular mechanism of proteolysis in Alzheimer's disease: progress toward therapeutic interventions. *Biochim. Biophys. Acta* **1751**, 60–67.

Hisanaga S. and Endo R. (2010) Regulation and role of cyclin-dependent kinase activity in neuronal survival and death. *J. Neurochem.* **115**, 1309–1321.

Hosokawa T., Saito T., Asada A., Ohshima T., Itakura M., Takahashi M., Fukunaga K. and Hisanaga S. (2006) Enhanced activation of Ca2+/calmodulin-dependent protein kinase II upon downregulation of cyclin-dependent kinase 5-p35. *J. Neurosci. Res.* **84**, 747–754.

Kusakawa G., Saito T., Onuki R., Ishiguro K., Kishimoto T. and Hisanaga S. (2000) Calpain-dependent proteolytic cleavage of the p35 cyclin-dependent kinase 5 activator ro p25. *J. Biol. Chem.* **275**, 17166–17172.

Lai K. O. and Ip N. Y. (2009) Recent advances in understanding the roles of Cdk5 in synaptic plasticity. *Biochim. Biophys. Acta* **1792**, 741–745.

Lee M. S., Kwon Y. T., Li M., Peng J., Friedlander R. M. and Tsai L. H. (2000) Neutoxicity induces cleavage of p35 to p25 by calpain. *Nature* **405**, 360–364.

Li C., Chen S., Yue P., Deng X., Lonial S., Khuri F. R. and Sun S. Y. (2010) Proteasome inhibitor PS-341 (bortezomib) induces calpain-dependent IkappaB (alpha) degradation. *J. Biol. Chem.* **285**, 16096–16104.

Liang B., Duan B. U., Zhou X. P., Gong J. X. and Luo Z. G. (2010) Calpain activation promotes BACE1 expression, amyloid precursor protein processing, and amyloid plaque formation in a transgenic mouse model of Alzheimer's diseases. *J. Biol. Chem.* **285**, 27737–27744.

Liu J., Liu M. C. and Wang K. K. (2008) Calpain in the CNS: from synaptic function to neurotoxicity. *Sci. Signal.* **1**, re1.

Maki M. and Hitomi K. (2000) Purification of recombinant calpastatin expressed in *Escherichia coli*. *Methods Mol. Biol.* **144**, 85–94.

Minegishi S., Asada A., Miyauchi S., Fuchigami T., Saito T. and Hisanaga S. I.. (2010) Membrane association facilitates degradation and

cleavage of the Cyclin-dependent kinase 5 activator p35 and p39. *Biochemistry* **49**, 5482–5493.

Moldoveanu T., Hosfield C. M., Lim D., Elce J. S., Jia Z. and Davies P. L. (2002) A Ca(2+) switch aligns the active site of calpain. *Cell* **108**, 649–660.

Murachi T. (1989) Intracellular regulatory system involving calpain and calpastatin. *Biochem. Int.* **18**, 263–294.

Nakajima R., Takao K., Huang S. M., Takano J., Iwata N., Miyakawa T. and Saido T. C. (2008) Comprehensive behavioral phenotyping of calpastatin-knockout mice. *Mol. Brain.* **1**, 7.

Ohshima T., Ward J. M., Huh C. G., Longencker G., Veeranna, Pant H. C., Ready R. O., Martin L. J. and Kulkarni A. B. (1996) Targeted disruption of the cyclin-dependent kinase 5 gene results in abnormal coticogenesis, neuronal pathology and perinatal death. *Proc. Natl Acad. Sci. USA* **93**, 11173–11178.

Ono K., Condron M. M. and Teplow D. B. (2010) Effects of the English (H6R) and Tottori (D7N) familial Alzheimer disease mutations on amyloid beta-protein assembly and toxicity. *J. Biol. Chem.* **285**, 23186–23197.

Otvos Jr. L., Feiner L., Lang E., Szendrei G. I., Goedert M. and Lee V. M. (1994) Monoclonal antibody PHF-1 recognizes tau protein phosphorylated at serine residues 396 and 404. *J. Neurosci. Res.* **39**, 669–673.

Patrick G. N., Zhou P., Kwon Y. T., Howley P. M. and Tsai L. H. (1998) p35, the neuronal-specific activator of cyclin-dependent kinase 5 (Cdk5) is degraded by the ubiquitin-proteasome pathway. *J. Biol. Chem.* **273**, 24057–24064.

Patrick G. N., Zukerberg L., Nikolic M., de la Monte S., Dikkes P. and Tsai L. H. (1999) Conversion of p35 to p25 deregulates Cdk5 activity and promotes neurodegeneration. *Nature* **402**, 615–622.

Pietsch M., Chua K. C. and Abell A. D. (2010) Calpains: attractive targets for the development of synthetic inhibitors. *Curr. Top. Med. Chem.* **10**, 270–293.

Plattner F., Angelo M. and Giese K. P. (2006) The roles of cyclin-dependent kinase 5 and glycogen synthase kinase 3 in tau hyperphosphorylation. *J. Biol. Chem.* **281**, 25457–25465.

Rao M. V., Mohan P. S., Peterhoff C. M. *et al.* (2008) Marked calpastatin (CAST) depletion in Alzheimer's disease accelerates cytoskeleton disruption and neurodegeneration: neuroprotection by CAST overexpression. *J. Neurosci.* **28**, 12241–12254.

Saido T. C., Sorimachi H. and Suzuki K. (1994) Calpain: new perspectives in molecular diversity and physiological-pathological involvement. *FASEB J.* **11**, 814–822.

Saito T., Ishiguro K., Onuki R., Nagai Y., Kishimoto T. and Hisanaga S. (1998) Okadaic acid-stimulated degradation of p35, an activator of CDK5, by proteasome in cultured neurons. *Biochem. Biophys. Res. Commun.* **252**, 775–778.

Saito T., Onuki R., Fujita Y., Kusakawa G., Ishiguro K., Bibb J. A., Kishimoto T. and Hisanaga S. (2003) Developmental regulation of

the proteolysis of the p35 cyclin-dependent kinase 5 activator by phosphorylation. *J. Neurosci.* **23**, 1189–1197.

Sato K., Zhu Y. S., Saito T., Yotsumoto K., Asada A., Hasegawa M. and Hisanaga S. (2007) Regulation of membrane association and kinase activity of Cdk5-p35 by phosphorylation of p35. *J. Neurosci. Res.* **85**, 3071–3078.

Strobl S., Fernandez-Catalan C., Braun M. *et al.* (2000) The crystal structure of calcium-free human m-calpain suggests an electrostatic switch mechanism for activation by calpain. *Proc. Natl Acad. Sci. USA* **97**, 588–592.

Suzuki K., Hata S., Kawabata Y. and Sorimachi H. (2004) Structure, activation, and biology of calpain. *Diabetes* **53**, S12–S18.

Takano J., Tomioka M., Tsubuki S., Highchi M., Iwata N., Itohara S., Maki M. and Saido T. C. (2005) Calpain mediates excitotoxic DNA fragmentation via mitochondrial pathway in adult brains. *J. Biol. Chem.* **280**, 16175–16184.

Tanaka K. (2009) The proteasome: overview of structure and functions. *Proc. Jpn. Acad. Ser. B Phys. Biol. Sci.* **85**, 12–36.

Taniguchi S., Fujita Y., Hayashi S., Kakita A., Takahashi H., Murayama S., Saido T. C., Hisanaga S., Iwatsubo T. and Hasegawa M. (2001) Calpain-mediated degradation of p35 to p25 in postmortem human and rat brains. *FEBS Lett.* **489**, 46–50.

Uchino H., Minamikawa-Tachino R., Kristián T., Perkins G., Narazaki M., Siesjö B. K. and Shibasaki F. (2002) Differential neuroprotection by cyclosporin A and FK506 following ischemia corresponds with differing abilities to inhibit calcineurin and the mitochondrial permeability transition. *Neurobiol. Dis.* **10**, 219–233.

Vaisid T., Kosower N. S., Katzav A., Chapman J. and Barnoy S. (2007) Calpastatin levels affect calpain activation and calpain proteolytic activity in APP transgenic mouse model of Alzheimer's disease. *Neurochem. Int.* **51**, 391–397.

Wei F. Y., Tomizawa K., Ohshima T. *et al.* (2005) Control of cyclin-dependent kinase 5 (Cdk5) activity by glutamatergic regulation of p35 stability. *J. Neurochem.* **93**, 502–512.

Wen Y., Yu W. H., Maloney B., Bailey J. *et al.* (2008) Transcriptional regulation of beta-secretase by p25/cdk5 leads to enhanced amyloidgenic processing. *Neuron* **57**, 680–690.

Xu W., Wong T. P., Chery N., Gaertner T., Wang Y. T. and Baudry M. (2007) Calpain-mediated mGluR1 alpha truncation: a key step in excitotoxicity. *Neuron* **53**, 399–412.

Yokota M., Saido T. C., Tani E., Kawashima S. and Suzuki K. (1995) Three distinct phases of fodrin proteolysis induced in postischemic hippocampus of calpain and unidentified protease. *Stroke* **10**, 1901–1907.

Zheng Y. L., Kesavapany S., Gravell M., Hamilton R. S., Schubert M., Amin N., Albers W., Grant P. and Pant H. C. (2005) A Cdk5 inhibitory peptide reduces tau hyperphosphorylation and apoptosis in neurons. *EMBO J.* **24**, 209–220.

PLoS one

Anti-Aβ Drug Screening Platform Using Human iPS Cell-Derived Neurons for the Treatment of Alzheimer's Disease

Naoki Yahata[1,2], Masashi Asai[2,3,4], Shiho Kitaoka[1,2], Kazutoshi Takahashi[1], Isao Asaka[1,2], Hiroyuki Hioki[2,5], Takeshi Kaneko[5], Kei Maruyama[3], Takaomi C. Saido[4], Tatsutoshi Nakahata[1], Takashi Asada[6], Shinya Yamanaka[1,7], Nobuhisa Iwata[2,4,8]*, Haruhisa Inoue[1,2,7]*

1 Center for iPS Cell Research and Application, Kyoto University, Kyoto, Japan, 2 Core Research for Evolutional Science and Technology, Japan Science and Technology Agency, Saitama, Japan, 3 Department of Pharmacology, Faculty of Medicine, Saitama Medical University, Saitama, Japan, 4 Laboratory for Proteolytic Neuroscience, RIKEN Brain Science Institute, Saitama, Japan, 5 Department of Morphological Brain Science, Graduate School of Medicine, Kyoto University, Kyoto, Japan, 6 Department of Neuropsychiatry, Institute of Clinical Medicine, University of Tsukuba, Tsukuba, Japan, 7 Yamanaka iPS Cell Special Project, Japan Science and Technology Agency, Saitama, Japan, 8 Graduate School of Biomedical Sciences, Nagasaki University, Nagasaki, Japan

Abstract

Background: Alzheimer's disease (AD) is a neurodegenerative disorder that causes progressive memory and cognitive decline during middle to late adult life. The AD brain is characterized by deposition of amyloid β peptide (Aβ), which is produced from amyloid precursor protein by β- and γ-secretase (presenilin complex)-mediated sequential cleavage. Induced pluripotent stem (iPS) cells potentially provide an opportunity to generate a human cell-based model of AD that would be crucial for drug discovery as well as for investigating mechanisms of the disease.

Methodology/Principal Findings: We differentiated human iPS (hiPS) cells into neuronal cells expressing the forebrain marker, Foxg1, and the neocortical markers, Cux1, Satb2, Ctip2, and Tbr1. The iPS cell-derived neuronal cells also expressed amyloid precursor protein, β-secretase, and γ-secretase components, and were capable of secreting Aβ into the conditioned media. Aβ production was inhibited by β-secretase inhibitor, γ-secretase inhibitor (GSI), and an NSAID; however, there were different susceptibilities to all three drugs between early and late differentiation stages. At the early differentiation stage, GSI treatment caused a fast increase at lower dose (Aβ surge) and drastic decline of Aβ production.

Conclusions/Significance: These results indicate that the hiPS cell-derived neuronal cells express functional β- and γ-secretases involved in Aβ production; however, anti-Aβ drug screening using these hiPS cell-derived neuronal cells requires sufficient neuronal differentiation.

Introduction

Alzheimer's disease (AD) is the most common cause of dementia in the elderly. It is characterized clinically by progressive declines in memory, executive function, and cognition. It is also characterized by pathological features, including the deposition of amyloid plaques and neurofibrillary tangles as well as neuronal and synaptic loss in particular areas of the brain [1]. Accumulation of amyloid β peptide (Aβ) is hypothesized to initiate the pathogenic cascade that eventually leads to AD. The amyloid hypothesis is based on an imbalance between the production and clearance of Aβ [2]. Aβ is produced by β- and γ-secretase-mediated sequential proteolysis of amyloid precursor protein (APP) and plays a central role in AD pathogenesis. Because β- and γ-secretases are directly involved in Aβ production, they are straightforward and attractive

therapeutic targets for AD. A number of compounds that inhibit or modulate these secretase activities and Aβ levels *in vitro* and *in vivo* have to date been developed [3,4].

Development of a human, cell-based *in vitro* assay system is a basic requisite for drug discovery and for investigating mechanisms of the disease. Induced pluripotent stem (iPS) cells reprogrammed from somatic cells [5,6] provide an opportunity to easily generate and use patient-specific differentiated cells. Because previous AD assay systems using human cancer cell lines or primary rodent cell cultures did not perfectly present the human intracellular environment or components, human iPS (hiPS) cell-derived neuronal cells may enable the development of more efficient drugs, such as γ-secretase modulators, and the better elucidation of AD mechanisms. In this study, we successfully generated forebrain neurons from hiPS cells, and showed that Aβ production in

neuronal cells was detectable and inhibited by some typical secretase inhibitors and modulators. Thus, we provide a new platform for AD drug development, which might be applied to AD patient-specific iPS cell research.

Results

Differentiation of forebrain neurons from hiPS cells

Recently, forebrain neurons were successfully differentiated from mouse embryonic stem (ES) cells [7,8,9] and human ES and/ or iPS cells [9,10,11]. The methods used for differentiation into spinal motor neurons and midbrain dopaminergic neurons required the morphogens retinoic acid (RA)/sonic hedgehog (SHH) and fibroblast growth factor 8 (FGF8)/SHH, respectively [11,12]. On the other hand, non-morphogens [10,11] or Lefty A and Dickkopf homolog 1 (Dkk1) [7,9] have been used for the induction of hiPS cells into forebrain neurons. Because amyloid plaques are observed in the cerebral cortex from the early stage of AD development [13], stem cells should be differentiated to at least forebrain neurons for *in vitro* assays in AD research.

We differentiated forebrain neurons from hiPS 253G4 cells, which were generated from human dermal fibroblasts using three reprogramming factors (Oct3/4, Sox2, and Klf4) [14], as described previously (Figure 1A) [12,15]. When neural stem cells were induced with Noggin and SB431542 for 17 days, we obtained cells that were positive for the neuroectodermal marker, Nestin (Figure 1B), as previously reported using human and monkey ES cells [15]. After culturing the cells with morphogen-free medium for days 17–24, Forkhead box G1 (Foxg1) expression was induced and Foxg1-positive cells were observed (Figure 1C, D) [11,15]. We also examined whether treatment with cyclopamine, an SHH inhibitor, increased the number of neurons presenting a glutamatergic phenotype as observed in mouse ES cells [8]. The expression level of vesicular glutamate transporter 1 (vGlut1), a glutamatergic marker, was not significantly increased by the addition of cyclopamine (final concentration 1 μM) from days 17 to 24 (data not shown). Therefore, we did not add cyclopamine in this period in subsequent experiments. At day 24, dissociated cells were reseeded on 24-well plates to further characterize the cells.

Next, we evaluated the hiPS cell-derived neuronal cells using four cortical layer-specific markers, T-brain-1 (Tbr1) and chicken ovalbumin upstream promoter transcription factor (COUP-TF)-interacting protein 2 (Ctip2) [9,10,11], and cut-like homeobox 1 (Cux1) and special AT-rich sequence-binding protein 2 (Satb2) [16]. Quantitative polymerase chain reaction (qPCR) revealed that expression levels of these markers were increased in a differentiation day-dependent manner (Figure 1E). At day 52, all four of these markers were visualized by immunocytochemistry (ICC) (Figure 1F). The percentages of marker-positive cells relative to the total number of cells were 62.2±2.9% for Tbr1, 11.9±3.0% for Ctip2, 82.6±5.0% for Cux1, and46.0±7.1% for Satb2. The population of each marker-positive cell was similar to that of data reported previously in human fetal brain around gestational week-20 [16]. In this experimental schedule, most cells expressed one or a few neocortical markers at day 52.

Characterization of hiPS cell-derived neuronal cells

Cells that were reseeded at day 24, were sparsely adhered to the culture plate and had proliferated and extended neurites in a time course-dependent manner as observed by the neuronal marker, class-III β-tubulin (Tuj1), and microtubule-associated protein 2 (MAP2) (Figure 2A). Tuj1 expression was almost saturated at day 45 (Figure 2B), but MAP2 and synapsin I expression were still increasing (Figure 2C, D). Synaptic development continued until

day 52, and many synapsin I-positive puncta were detected by ICC at day 52 (Figure 2A). Expression of the glial marker, glial fibrillary acidic protein (GFAP), was highest at day 52 in this schedule (Figure 2E). This sequential expression pattern is similar to that reported recently in human pluripotent stem cell-derived neurons; the synapsin I-positive neuronal and GFAP-positive glial cultures at day 52 corresponded to the stage at which spontaneous neuronal activity was observed [17].

We then examined the neurotransmitter phenotypes of these differentiated neurons by evaluating the synthesizing enzymes for two typical cortical neurotransmitters, glutamate and γ-aminobutyric acid (GABA). Expression of the glutamatergic neuronal marker, phosphate-activated glutaminase (PAG) [18], and the GABAergic neuronal marker, glutamate decarboxylase (GAD), were observed by ICC at day 52 (Figure 2F). PAG- and GAD-positive neurons comprised 60±20% and 5±4% of total cells, respectively. Most of the Tuj1-positive neurons were also co-localized with the punctate signals of vGlut1 (Figure 2G). GABA-positive neurons comprised a similar population to the GAD-positive ones (Figure 2F, H). On the other hand, cholineacetyl-transferase (ChAT) or vesicular acetylcholine transporter (VAChT)-positive cholinergic neurons were little observed at day 52, although their mRNA level increased with differentiation time (Figure S1). These data showed that a majority of differentiated neuronal cells possessed a glutamatergic phenotype in the present condition.

Differentiated neuronal cells express some components related to Aβ production

To evaluate their usefulness as an AD model, we measured the levels of Aβ secreted from the differentiated neuronal cells at days 38, 45, and 52. In the non-amyloidogenic pathway, α-secretase cleaves full-length APP (FL-APP) within the Aβ domain to the large soluble APP fragment (sAPPα) and APP-C terminal fragment α (CTFα) (Figure 3) [19]. In the amyloidogenic pathway, β-secretase, β-site APP cleaving enzyme 1 (BACE1), cleaves APP on the N-terminal side of the Aβ domain to soluble sAPPβ and APP-CTFβ (Figure 3). FL-APP and its cleavage products were increased in a time-course-dependent manner (Figure 3).

APP has three alternatively spliced isoforms: APP695, APP751, and APP770. APP695 is most abundantly expressed in neurons, whereas APP751 and APP770 show more ubiquitous expression patterns [20]. In cell lysates, we detected three separate APP variants on western blots. The estimated percentages of the neuron-dominant variant APP695 were 64.5±1.0%, 68.6±2.2%, and 69.6±2.1% at days 38, 45, and 52, respectively (Figures 3A and S2). The neuronal population at day 52 was approximately consistent with the sum of the percentages of the glutamatergic and GABAergic neurons mentioned above.

The aspartyl protease BACE1, the major β-secretase involved in cleaving APP, is a significant molecule for AD pathology because BACE1 protein levels and activity are increased in the brains of patients with the sporadic form of AD [21]. In our differentiated neurons, BACE1 protein levels were increased in a time course-dependent manner (Figure 4A, B), and we speculated that the upregulation of BACE1 protein levels may be due to a posttranscriptional mechanism [22]. BACE1 mRNA levels were slightly elevated with time (Figure 4B). These data may indicate that increased BACE1 protein levels were mainly induced by translational activation along with neuronal differentiation.

APP-CTFβ is cleaved to Aβ and APP intercellular domain (AICD) by γ-secretase (Figure 3). The γ-secretase complex consists of four core members, presenilin (PS; either PS1 or PS2), nicastrin, Pen-2, and Aph-1 [23]. PS1, nicastrin, and Pen-2 were detected by
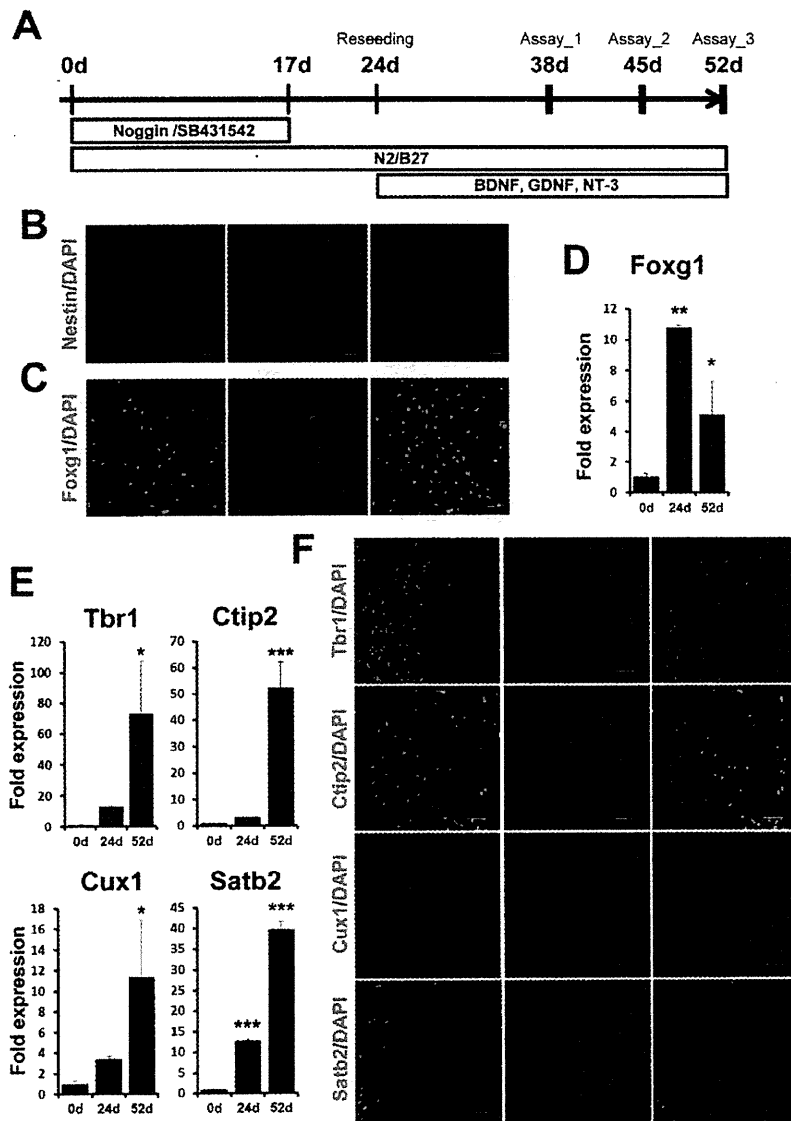
Figure 1. Differentiation of forebrain neurons from hiPS cells. (A) Experimental scheme of neural differentiation from hiPS cells, 253G4. Nestin-positive neuroepithelial cells (B) and Foxg1-positive cells (C) were observed at days 17 and 24, respectively. Scale bar, 50 μm. Expression levels of Foxg1 (D) and the neocortical markers Tbr1, Ctip2, Cux1, and Satb2 (E) at days 0, 24, and 52. Expression levels were measured by qPCR and normalized by that of GAPDH. "Fold expression" is shown as a ratio of day 24/day 0 or day52/day 0. Each column represents the mean ± SD of 3 assays. $^*p<0.05$, $^{**}p<0.01$, $^{***}p<0.001$, significantly different from day 0 by Dunnett's test. (F) ICC staining of Tbr1-, Ctip2-, Cux1- and Satb2-positive cells at day 52. Scale bar, 50 μm.
doi:10.1371/journal.pone.0025788.g001

western blotting, but their expression levels did not change markedly over time (Figure 4A, C). Aph-1 has two isoforms in human, Aph-1A and Aph-1B, which are considered to have different effects on the production of Aβ species related to AD [24]. Their expression levels measured by qPCR were relatively constant (Figure 4D). The Aph-1B/Aph-1A ratios also did not show significant differences among the time points analyzed here (Figure 4E).

Aβ has several species, including Aβ40 and Aβ42, which have emerged as two of the most robust Aβ measurements in brain. Recent studies suggest that Aβ40 and Aβ42 may have different effects on Aβ aggregation or oligomerization [25,26]. We

measured Aβ40 and Aβ42 secreted into conditioned media for 2 days by sandwich ELISA. Both types of Aβ increased with time (Figure 5A). The level of Aβ40 was higher than that of Aβ42, compatible with previous reports [4,27,28,29,30]. Interestingly, the ratio of Aβ42/Aβ40 was highest at day 38, and there was no significant difference between days 45 and 52 (Figure 5B).

Inhibition of Aβ40 and Aβ42 secretion

We examined whether the differentiated neurons contained funtional β- and γ-secretases and whether Aβ secretion could be controlled. We selected the most effective, commercially available β- and γ-secretase inhibitors, β-secretase inhibitor IV (BSI) [31]
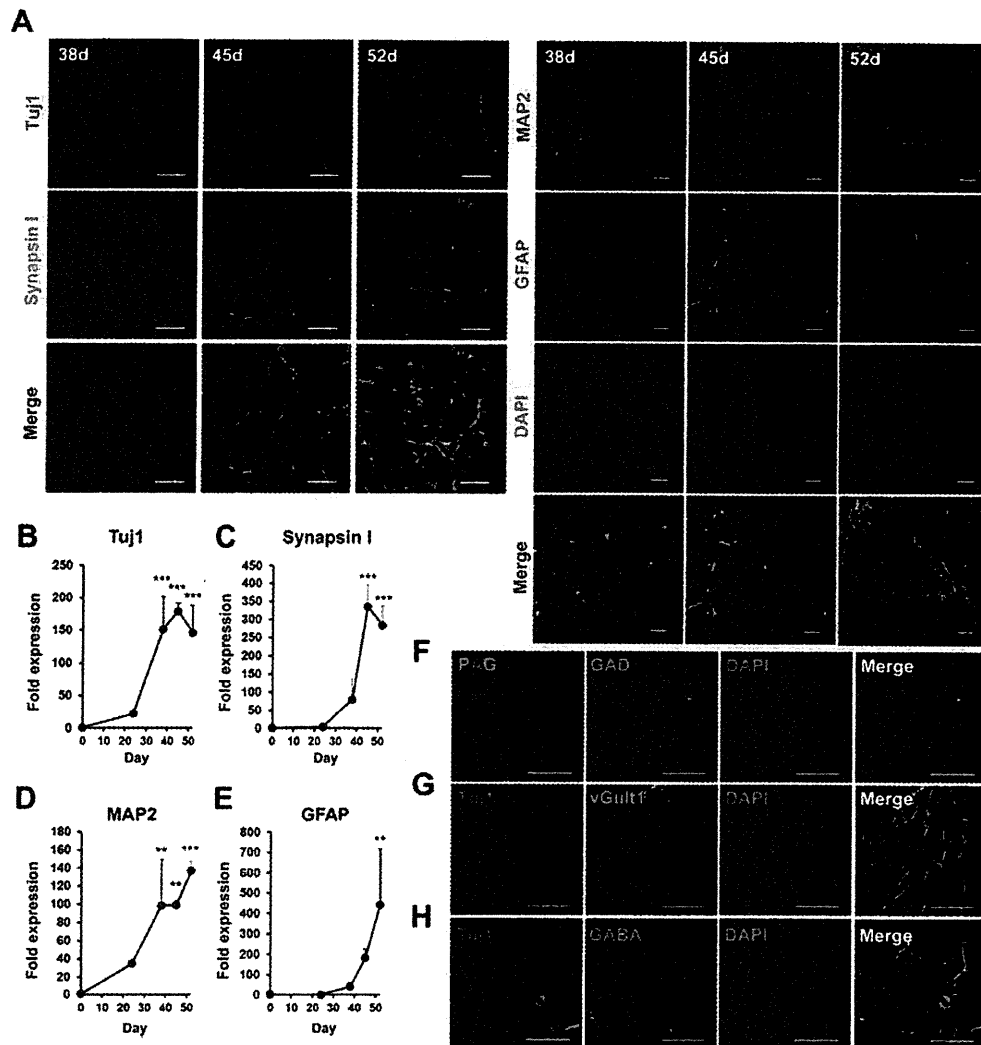
Figure 2. Characterization of neuronal and glial cells differentiated from hiPS cells. (A) Time-dependent morphological changes of cells reseeded in a 24-well plate. Neuronal and glial cells were stained by anti-Tuj1 (left; red), anti-synapsin I (left; green), anti-MAP2 (right; red), and anti-GFAP (right; green) antibodies and DAPI (right; blue) at 38, 45, and 52 days. Scale bar, left; 20 μm, right; 50 μm. Expression levels of Tuj1 (B), synapsin I (C), MAP2 (D), and GFAP (E) at days 0, 24, 38, 45, and 52 were measured by qPCR and normalized by that of GAPDH. "Fold expression" is the ratio of expression at each day compared to day 0. Each point represents mean ± SD of 3 assays. $^{*}p<0.05$, $^{**}p<0.01$, $^{***}p<0.001$, significantly different from day 0 by Dunnett's test. (F–H) Neurotransmitter phenotypes at day 52. PAG (red)- and GAD (green)-positive (F), vGlut1 (green)- and Tuj1 (red)-positive (G), and GABA (green)- and Tuj1 (red)-positive cells (H). Blue, DAPI. Scale bar, 50 μm.
doi:10.1371/journal.pone.0025788.g002

and γ-secretase inhibitor XXI/Compound E (GSI) [32], respectively. We also examined the effect of a non-steroidal anti-inflammatory drug (NSAID), sulindac sulfide [33], because some NSAIDs directly modulate γ-secretase activity to selectively lower Aβ42 levels [33,34]. The cells were treated with each drug for 2 days, and Aβ was monitored in the collected media at day 38 or 52.

There were different susceptibilities to all three drugs between days 38 and 52 (Figure 6) as revealed by two-way analysis of variance (ANOVA) [significant interaction between day and dose (BSI, $p<0.001$ in Aβ40 and Aβ42, respectively; GSI, $p<0.001$ in Aβ40 and Aβ42, respectively; NSAID, $p<0.001$ in Aβ42)]. Following BSI and NSAID treatment, secretion of Aβ40 and

Aβ42 was decreased in a dose-dependent manner (Figure 6A, B, E, and F). NSAID especially showed more efficient inhibition of Aβ42 than that of Aβ40, consistent with a previous report [33]. Following GSI treatment (Figure 6C, D), secretion of both Aβ40 and Aβ42 was increased at lower doses (10^{-11}–10^{-8} M), but was inhibited at higher doses (10^{-7}–10^{-6} M) at day 52. This phenomenon, which is called a "gradual Aβ rise", was observed following the addition of other GSIs in a cell line system [35]. On the other hand, secretion of both Aβ40 and Aβ42 at day 38 showed a fast increase at lower doses (10^{-11}–10^{-9} M) (Aβ surge) and drastic decline at 10^{-8} M. We also examined the effects of these inhibitors on cell viability using the lactate dehydrogenase (LDH) assay. Two-day-treatments with the highest concentrations

A

B
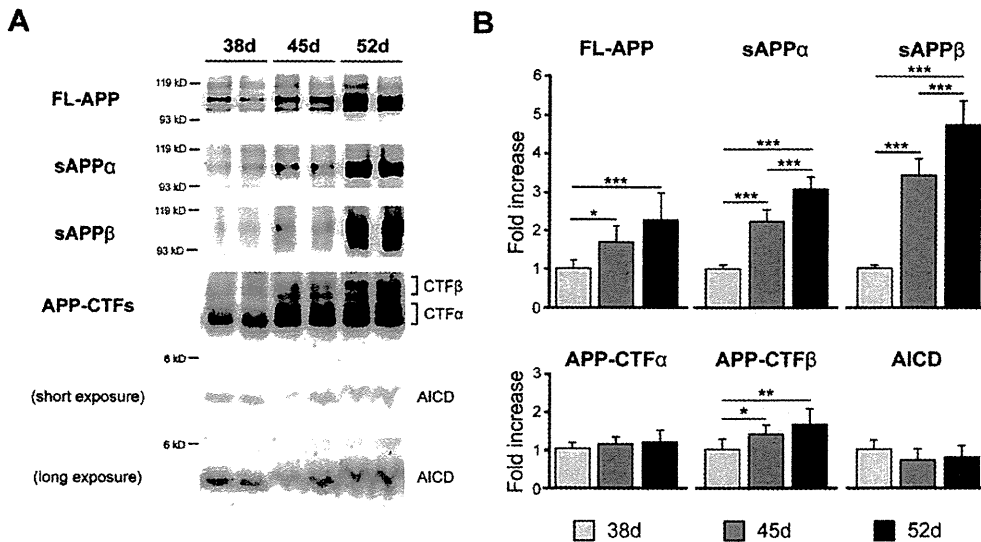
Figure 3. APP was expressed in hiPS cell-derived neuronal cells. HiPS cell-derived neuronal cells express full-length APP, sAPPα, sAPPβ, APP-CTFα, APP-CTFβ and AICD at 38, 45, and 52 days. (A) Representative western blots of APP and its fragments. (B) Each column represents mean ± SD of 8 samples measured by quantitative western blot analysis and normalized by that of β-actin. "Fold expression" represents the ratio of expression on the given day compared to day 38. $^*p<0.05$, $^{**}p<0.01$, $^{***}p<0.001$, Tukey's test.
doi:10.1371/journal.pone.0025788.g003

of BSI, GSI, or NSAID did not induce cell death (Table S1). We also traced these experiments using human ES (hES) cell (H9)-derived neuronal cells (Figure S4) because remaining expression of reprogramming factors, Oct3/4 and Klf4, were observed in hiPS cell (253G4)-derived neuronal cells (Figure S6). The Aβ production and its inhibition by these drugs in hES cell-derived neuronal cells were relatively similar to those in hiPS cell-derived ones (Figure S5). These data showed that BSI, GSI, and NSAID partially or fully blocked Aβ production in the hiPS cell-derived neuronal cells, indicating that these cells expressed functional β- and γ-secretases.

Discussion

AD is the most common cause of dementia in the elderly, with progressive neuronal loss in the cerebral cortex and hippocampal formation. Although the underlying etiology of most AD remains unclear, Aβ is thought to play a pivotal role in its pathogenesis. Studies from animal and cellular models have shown that mutations in the APP, PS1, and PS2 genes affected the production of Aβ, which contributes to the formation of amyloid plaques [19]. In several strains of mouse models, Aβ levels in brain tissue, cerebrospinal fluid (CSF), and plasma have been associated with AD pathogenesis and cognitive impairment [27,28,36]. Human samples from clinical AD patients have also been used for pathological and biochemical analyses to understand the etiology of AD. Aβ levels in CSF and plasma have been examined to evaluate their risks for AD [29,37], but brain tissues are only available postmortem for such analyses. On the other hand, immortalized human cell lines derived from kidney or brain, primary neurons derived from mice and rats, or cells artificially overexpressing APP or presenilin with or without familial AD mutations have been utilized for in vitro studies [4,30]. There is no doubt that these cells are quite different from living neurons in the human body in terms of innate qualities. Although we have had no choice until recently, important advances in technology of iPS cells

may now provide the opportunity to use intact human-derived neuronal cells [38].

We evaluated whether iPS cell-derived neuronal cells could be applied to an in vitro cell-based assay system for AD research. In particular, further investigations into the metabolic mechanisms of Aβ are requisite for drug development to treat the brains of patients afflicted with AD. In this respect, we provide a profile of the molecular components associated with Aβ production in hiPS cell-derived neuronal cells and propose to add an Aβ assay system using these cells to the panel of generalized Aβ-monitoring systems (Table 1). Human neuronal cells are considered to provide more accurate human neuronal conditions within which to evaluate drug efficacy or toxicity than other human cell lines (e.g., cancer lines). Furthermore, we would be able to investigate how hiPS cell-derived neuronal cells reflect AD-related physiological and pathological conditions based on Aβ production.

In the present study, we characterized iPS cell-derived neuronal cells in terms of their expression of neuronal and glial markers by exposing them to Noggin and SB431542 during their differentiation (Figures 1 and 2). We observed increases in GFAP mRNA levels and in synapsin I-positive synaptic puncta at day 52. This was consistent with data showing that the existence of astrocytes promotes synaptic activity in human ES cell-derived neurons [40]. When differentiation occurred in the presence of non-morphogens, we obtained mainly glutamatergic neurons (Figure 2F, G), quite in line with previous reports of concerning hES and hiPS cells [10,11]. Expression of the forebrain marker Foxg1 suggests a default forebrain identity of the 253G4 iPS cells used in this study (Figure 1C, D). We also observed the expression of the neocortex-specific transcriptional factors Tbr1, Ctip2, Cux1, and Satb2 (Figure 1E, F). These expression schemes appear to mimic human neocortical development in vitro [16], although further analyses are needed to assist in understanding human neuronal subtype-specific differentiation.

This is the first study to observe the expression of APP, β- and γ-secretase, and the production of Aβ in hiPS cell-derived neuronal